



Search for a heavy pseudoscalar Higgs boson decaying into a 125 GeV Higgs boson and a Z boson in final states with two tau and two light leptons at $\sqrt{s} = 13$ TeV

The CMS Collaboration*

Abstract

A search is performed for a pseudoscalar Higgs boson, A , decaying into a 125 GeV Higgs boson h and a Z boson. The h boson is specifically targeted in its decay into a pair of tau leptons, while the Z boson decays into a pair of electrons or muons. A data sample of proton-proton collisions collected by the CMS experiment at the LHC at $\sqrt{s} = 13$ TeV is used, corresponding to an integrated luminosity of 35.9 fb^{-1} . No excess above the standard model background expectations is observed in data. A model-independent upper limit is set on the product of the gluon fusion production cross section for the A boson and the branching fraction to $Zh \rightarrow \ell\ell\tau\tau$. The observed upper limit at 95% confidence level ranges from 27 to 5 fb for A boson masses from 220 to 400 GeV, respectively. The results are used to constrain the extended Higgs sector parameters for two benchmark scenarios of the minimal supersymmetric standard model.

"Published in the Journal of High Energy Physics as doi:10.1007/JHEP03(2020)065."

1 Introduction

In the standard model (SM) [1–3], the Brout–Englert–Higgs mechanism [4–9] is responsible for the electroweak symmetry breaking, and it predicts the existence of the Higgs boson. A Higgs boson with a mass around 125 GeV was discovered by the ATLAS and CMS Collaborations in 2012 [10–12]. The best measurement of the Higgs boson mass to date, 125.26 ± 0.21 GeV, comes from a partial Run 2 data set analysis by the CMS Collaboration [13]; the result is consistent with the earlier Run 1 combined measurement by the ATLAS and CMS Collaborations [14] and the recent results by the ATLAS Collaboration [15]. The couplings of the observed boson have been studied extensively, and are found to be compatible with the SM expectation [16, 17].

The observation of the Higgs boson has not only given closure to the search for particles described by the SM, but also constrains the beyond-the-SM theories proposed to explain some of the open questions in particle physics. A class of simple extensions of the SM, two-Higgs-doublet models (2HDMs), predicts the existence of five Higgs bosons [18, 19]. Two of these five particles are CP-even Higgs bosons (h and H), and thus either of them could correspond to the observed particle. The properties of the observed state can be used to exclude regions of the parameter space of 2HDMs. Further constraints can be placed by performing searches for the four additional Higgs bosons, namely the scalar H, the CP-odd Higgs boson A, and two charged Higgs bosons H^\pm . Moreover, 2HDMs are a prerequisite for the minimal supersymmetric standard model (MSSM) where the extended Higgs sector at tree-level is fully defined by two parameters, conventionally chosen to be the ratio of the vacuum expectation values of the two Higgs doublets ($\tan \beta$) and the mass of the pseudoscalar A (m_A).

In the MSSM, given that the mass of the h boson is as large as 125 GeV, the scale of the soft supersymmetry breaking masses can be larger than 1 TeV. This is a reasonable assumption based on the nonobservation of supersymmetric particles at the CERN LHC thus far. In many of the MSSM benchmark scenarios typically studied, the predicted mass of the Higgs boson is lower than 125 GeV in the low $\tan \beta$ region [20]. We study two MSSM benchmark scenarios that can accommodate these constraints in most of the m_A – $\tan \beta$ plane: $M_{h,\text{EFT}}^{125}$ [20] and hMSSM [21–24]. The Higgs sector predictions of the $M_{h,\text{EFT}}^{125}$ scenario are derived from a 2HDM effective field theory framework, with a supersymmetric mass scale that can reach up to 10^{16} GeV, in order for the Higgs boson mass to be compatible with 125 GeV in the low $\tan \beta$ region. In the hMSSM scenario, by requiring $m_h = 125$ GeV, the dominant radiative corrections to the Higgs boson mass become fixed, which are then used to determine the masses and couplings of the other Higgs bosons.

The parameter spaces of these benchmark scenarios can be explored by studying processes producing an experimentally accessible signature with a 125 GeV Higgs boson. One such process is the decay of the A boson into a 125 GeV Higgs boson and a Z boson. In the parameter space region with low $\tan \beta$ values, this decay has a substantial branching fraction. For $\tan \beta \lesssim 5$ the A boson is produced mainly in gluon fusion ($gg \rightarrow A$), but for higher $\tan \beta$ values the associated production with b quarks ($b\bar{b}A$) becomes dominant. The Feynman diagrams for both production processes are shown in Fig. 1.

This paper reports on a search for the pseudoscalar A boson decaying into a 125 GeV Higgs boson h and a Z boson in proton-proton (pp) collisions at $\sqrt{s} = 13$ TeV. The search is based on a data set collected in 2016 by the CMS experiment, corresponding to an integrated luminosity of 35.9 fb^{-1} . The analysis is primarily sensitive to the assumed gluon fusion production of the A boson, but the associated production with b quarks is included in the interpretation of the results. The studied signal mass range begins at 220 GeV because the A boson must be massive

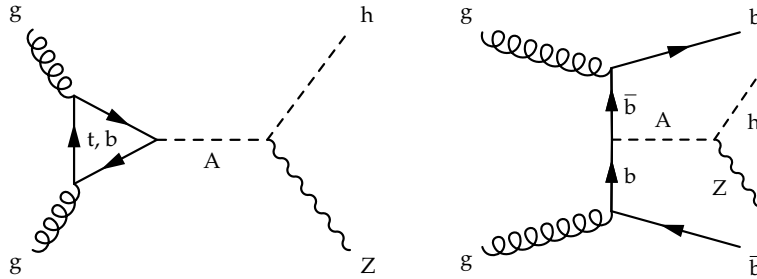


Figure 1: Feynman diagrams for two dominant production processes for the pseudoscalar A boson: gluon fusion (left) and associated production with b quarks (right). In both cases the A boson decays into a 125 GeV Higgs boson and a Z boson.

enough to decay into the considered Zh state. The mass range extends up to 400 GeV, slightly above where the mass of the A boson exceeds twice the top quark mass. In this region the $A \rightarrow t\bar{t}$ decay channel is expected to dominate.

Previous searches for the $A \rightarrow Zh$ process, performed by the ATLAS and CMS Collaborations, considered a final state with two tau leptons from the h boson decay, and used data sets collected in pp collisions at $\sqrt{s} = 8$ TeV [25, 26]. The ATLAS and CMS Collaborations have also searched for the pseudoscalar A decaying into the same intermediate Zh state but with the Higgs boson h decaying into a pair of bottom quarks in pp collisions at $\sqrt{s} = 13$ TeV [27, 28]. These analyses set both model-independent and model-dependent limits in the context of 2HDMs.

In this search, the Higgs boson is sought in its decay into a pair of tau leptons. Four possible $\tau\tau$ decay channels of the Higgs boson are considered: $e\tau_h$, $\mu\tau_h$, $\tau_h\tau_h$, and $e\mu$, where τ_h denotes a tau lepton decaying hadronically. Throughout the paper, neutrinos are omitted from the notation of the final states. These four decay channels are combined with the Z boson decays into two light leptons, i.e., $Z \rightarrow \ell^+\ell^-$ ($\ell = e, \mu$), resulting in eight distinct final states of the A boson decay. To account for the missing transverse momentum that results from the neutrinos in the final states, we use the SVFIT algorithm [29] to reconstruct the four-vector of the Higgs boson while constraining its mass to 125 GeV. Compared to the previous result presented by the CMS Collaboration [26], this novel approach significantly increases the sensitivity of the search.

2 The CMS detector

The central feature of the CMS apparatus is a superconducting solenoid of 6 m internal diameter, providing a magnetic field of 3.8 T. Within the solenoid volume are a silicon pixel and strip tracker, a lead tungstate crystal electromagnetic calorimeter (ECAL), and a brass and scintillator hadron calorimeter, each composed of a barrel and two endcap sections. Forward calorimeters extend the pseudorapidity (η) coverage provided by the barrel and endcap detectors. Muons are detected in gas-ionization chambers embedded in the steel flux-return yoke outside the solenoid. Events of interest are selected using a two-tiered trigger system [30]. The first level (L1), composed of custom hardware processors, uses information from the calorimeters and muon detectors to select events at a rate of around 100 kHz within a time interval of less than 4 μ s. The second level, known as the high-level trigger (HLT), consists of a farm of processors running a version of the full event reconstruction software optimized for fast processing, and reduces the event rate to around 1 kHz before data storage. A more

detailed description of the CMS detector, together with a definition of the coordinate system used and the relevant kinematic variables, can be found in Ref. [31].

3 Simulated samples and models

Simulated signal events with a pseudoscalar Higgs boson A produced in gluon fusion ($gg \rightarrow A$), decaying into a 125 GeV Higgs boson and a Z boson and finally into two tau and two leptons (electrons or muons) are generated at leading order (LO) using `MADGRAPH5_aMC@NLO v2.4.2` [32]. The considered A boson mass points are within 220–400 GeV, as in this mass range the $A \rightarrow Zh$ decay becomes predominant. The samples are based on the $m_h^{\text{mod}+}$ model [33], assuming a low value of $\tan\beta$ (~ 2). The generated width of the A boson is small compared to the instrumental resolution for all masses. Additional signal events are simulated for a 300 GeV A boson produced in association with b quarks ($b\bar{b}A$) and are used only to study the selection efficiency, necessary for setting model-dependent limits, as explained in Section 8.

The background processes consist of all SM processes with nonnegligible yield in the studied final states, including the Higgs boson production through processes predicted in the SM (e.g. Zh , Wh , $t\bar{t}h$). The background processes with a Higgs boson decaying into two tau leptons, produced in association with a W or Z boson (Wh or Zh), are generated at next-to-LO (NLO) in perturbative quantum chromodynamics (QCD) with the `POWHEG 2.0` [34–38] generator extended with the `MinLO` procedure [39]. The contribution from Higgs boson events produced via gluon fusion or vector boson fusion and decaying into two tau leptons is negligible. The transverse momentum (p_T) distribution of the Higgs boson in the `POWHEG` simulations is tuned to match closely the next-to-NLO (NNLO) plus next-to-next-to-leading-logarithmic prediction in the `HRES 2.3` generator [40, 41]. The production cross sections and branching fractions for the SM Higgs boson production and their corresponding uncertainties are taken from Refs. [42–44].

The background samples for $t\bar{t}h$, $t\bar{t}$, WZ , and $qq \rightarrow ZZ$, as well as $Wh \rightarrow WWW$, $Wh \rightarrow WZZ$, $Zh \rightarrow ZWW$, $Zh \rightarrow ZZZ$, and $gg \rightarrow h \rightarrow ZZ$ processes, are generated at NLO with `POWHEG 2.0`. The $gg \rightarrow ZZ$ process is generated at LO with `MCFM` [45]. Samples for the $qq \rightarrow ZZ$ and $gg \rightarrow ZZ$ processes include all SM events with two Z bosons in the final states except the ones from the $gg \rightarrow h \rightarrow ZZ$ process. The `MADGRAPH5_aMC@NLO 2.2.2` or `2.3.3` generator is used for triboson, Z + jets, $t\bar{t}W$, and $t\bar{t}Z$ production, with the jet matching and merging scheme applied either at NLO with the `FxFx` algorithm [46] or at LO with the `MLM` algorithm [47]. The generators are interfaced with `PYTHIA 8.212` [48] to model the parton showering and fragmentation, as well as the decay of the tau leptons. The `PYTHIA` parameters affecting the description of the underlying event are set to the `CUETP8M1` tune [49]. The set of parton distribution functions (PDFs) used in the simulation is `NNPDF3.0` [50].

The generated events are processed through a simulation of the CMS detector based on `GEANT4` [51], and are reconstructed with the same algorithms that are used for data. The simulated samples include additional pp interactions per bunch crossing, referred to as in-time pileup. The effect of inelastic collisions happening in the preceding and subsequent bunch crossings (out-of-time pileup) is also considered. The effect of pileup is taken into account by generating concurrent minimum bias collision events. The simulated events are weighted such that the distribution of the number of pileup interactions matches with that observed in data. The pileup distribution is estimated from the measured instantaneous luminosity for each bunch crossing, resulting in an average of approximately 23 interactions per bunch crossing.

To produce model-dependent interpretations of the results described in Section 8, we utilize

production cross section and branching fraction calculations for the pseudoscalar A in the $M_{h,\text{EFT}}^{125}$ and hMSSM scenarios. In the $M_{h,\text{EFT}}^{125}$ scenario, Higgs boson masses and mixing parameters (and effective Yukawa couplings) were calculated with a yet unpublished version of FEYNHIGGS based on version 2.14.3 [20, 52–56].

For the gluon-gluon fusion process in the $M_{h,\text{EFT}}^{125}$ (hMSSM) scenario, inclusive cross sections are obtained with SUSHI 1.7.0 (1.4.1) [57, 58], which includes supersymmetric NLO QCD corrections [59–64], NNLO QCD corrections for the top quark contribution in an effective theory of a heavy top quark [65–69] and electroweak effects from light quarks [70, 71].

Inclusive $b\bar{b}A$ production cross sections at NNLO QCD accuracy in the five-flavor scheme are calculated with SUSHI, based on BBH@NLO [72]. The results are combined with the $b\bar{b}A$ cross section calculation at NLO in QCD in the four-flavor scheme [73, 74] using the Santander matching scheme [75] for the hMSSM scenario, and matched predictions [76–79] for the $M_{h,\text{EFT}}^{125}$ scenario.

In the hMSSM scenario, branching fractions are solely computed with HDECAY 6.40 [80–82], whereas the $M_{h,\text{EFT}}^{125}$ scenario relies on a yet unpublished version of FEYNHIGGS based on version 2.14.3 [20, 52–56].

4 Event reconstruction

Both observed and simulated events are reconstructed using the particle-flow (PF) algorithm [83]. The particle-flow algorithm aims to reconstruct and identify each individual particle in an event, with an optimized combination of information from the various elements of the CMS detector. In this process the reconstructed PF objects include photons, electrons, muons, neutral hadrons, and charged hadrons.

Higher-level objects are reconstructed from combinations of the PF objects. For example, jets are reconstructed with an anti- k_T clustering algorithm implemented in the FASTJET library [84, 85]. The reconstruction is based on the clustering of PF objects with a distance parameter of 0.4. Charged PF objects are required to be associated with the primary vertex of the interaction. The reconstructed vertex with the largest value of summed physics-object p_T^2 is taken to be the primary pp interaction vertex. The physics objects are the jets, clustered using the jet finding algorithm [84, 86] with the tracks assigned to the vertex as inputs, and the associated missing transverse momentum, taken as the negative vector sum of the p_T of those jets. Jet energy corrections are derived from simulation studies so that the average measured response of jets becomes identical to that of particle level jets. In situ measurements of the momentum balance in dijet, photon+jet, Z + jet, and multijet events are used to determine any residual differences between the jet energy scale in data and in simulation, and appropriate corrections are applied [87].

While neutrinos cannot be detected directly, they contribute to the missing transverse momentum. The missing transverse momentum vector \vec{p}_T^{miss} is computed as the negative vector sum of the transverse momenta of all the PF objects in an event [88]. The \vec{p}_T^{miss} is modified to account for corrections to the energy scale of the reconstructed jets in the event.

Electrons are identified by a multivariate analysis (MVA) discriminant that requires as input several quantities describing the track quality, the shapes of the energy deposits in the ECAL, and the compatibility of the measurements from the tracker and the ECAL [89]. Muon identification relies on the number of hits in the inner tracker and the muon systems, and on the quality of the reconstructed tracks [90]. Electrons and muons selected in this analysis are

required to be consistent with originating from the primary vertex.

A lepton isolation discriminant I^ℓ is defined to reject nonprompt or misidentified leptons ($\ell = e, \mu$):

$$I^\ell \equiv \frac{\sum_{\text{charged}} p_T + \max\left(0, \sum_{\text{neutral}} p_T - \frac{1}{2} \sum_{\text{charged, PU}} p_T\right)}{p_T^\ell}, \quad (1)$$

where p_T^ℓ stands for the p_T of the lepton. The variable $\sum_{\text{charged}} p_T$ is the scalar sum of the transverse momenta of the charged particles originating from the primary vertex and located in a cone of size $\Delta R = \sqrt{(\Delta\eta)^2 + (\Delta\phi)^2} = 0.3(0.4)$ centered on the electron (muon) direction, where ϕ is the azimuthal angle in radians. The sum $\sum_{\text{neutral}} p_T$ represents a similar quantity for neutral particles. The scalar sum of the transverse momenta of charged hadrons originating from pileup vertices in the cone, $\sum_{\text{charged, PU}} p_T$, is used to estimate the contribution of photons and neutral hadrons originating from pileup vertices. The factor of 1/2 corresponds approximately to the ratio of neutral- to charged-hadron production in the hadronization process of inelastic pp collisions. The isolation requirements based on I^ℓ are described in the following section.

The combined secondary vertex algorithm [91] is used to identify jets that are likely to have originated from a bottom quark (“b-tagged jets”). In this algorithm, the secondary vertices associated with the jet and the track-based lifetime information are given as inputs to an MVA discriminant designed for b jet identification. Differences in the b tagging efficiency between data and simulation are taken into account by applying a set of p_T -dependent correction factors to the simulated events [91]. The identification efficiency for genuine b jets in this analysis is approximately 63%, whereas the misidentification probability for c (light-flavor or gluon) jets is approximately 12 (0.9)% for jet $p_T > 20$ GeV.

Anti- k_T jets seed the hadron-plus-strips algorithm [92, 93] which is used to reconstruct τ_h candidates. A hadronic decay of a tau lepton can result in one or more charged hadrons, and additional π^0 particles. These π^0 s are reconstructed by clustering electromagnetic deposits in the ECAL into “strips” in the η - ϕ plane. The strips are elongated in the ϕ direction to contain the calorimeter signatures of converted photons from neutral pion decays. The algorithm reconstructs τ_h candidates based on the number of tracks and the number of strips representing the number of charged hadrons (“prongs”) and the number of π^0 s present in the decay. The τ_h candidates used in this analysis are reconstructed in three decay modes: 1-prong, 1-prong+ π^0 s, and 3-prong.

To suppress objects (jets and leptons) misidentified as τ_h candidates, an MVA discriminant [93] including calorimetric information, isolation sums, and lifetime information is used. A misidentification rate for quark- and gluon-initiated jets of less than 1% is achieved within a p_T range typical of a τ_h candidate originating from an h boson. At the same time, an efficiency for selecting τ_h candidates of $\approx 70\%$ can be achieved for τ_h candidates passing the decay mode reconstruction discussed above. To further suppress electrons and muons misidentified as τ_h candidates, dedicated criteria based on the consistency between the measurements in the tracker, the calorimeters, and the muon detectors are applied [92, 93]. The τ_h energy scale is measured from $Z \rightarrow \tau\tau$ events and the correction is propagated to the simulation for each decay mode. A “tag-and-probe” measurement [93] in $Z \rightarrow \ell\ell$ events, where one of the ℓ is misidentified as a τ_h candidate, is used to correct the energy scale of electrons and muons misidentified as τ_h candidates in simulation.

The reconstructed mass of the A boson candidate can be used to discriminate between signal- and background-like events. Multiple reconstruction methods are considered and described

below. The resulting mass distributions for the signal process ($m_A = 300 \text{ GeV}$) are shown in Fig. 2. The shapes of the background distributions do not depend on the mass reconstruction method as strongly as the shape of the signal distribution. The simplest reconstructed mass, $m_{\ell\ell\tau\tau}^{\text{vis}}$, uses only the visible decay products and combines the reconstructed $Z \rightarrow \ell\ell$ four-vector with the $h \rightarrow \tau\tau$ four-vector based only on visible τ decay products. The resulting mass resolution for $m_{\ell\ell\tau\tau}^{\text{vis}}$ is approximately 15% for an A boson with a mass of 300 GeV in all final states.

The mass resolution of the reconstructed A boson candidate can be significantly improved by accounting for the neutrinos associated with the leptonic and hadronic tau decays. We use the SVFIT algorithm [29] to estimate the mass of the Higgs boson, denoted as $m_{\tau\tau}^{\text{fit}}$. The SVFIT algorithm combines the \vec{p}_T^{miss} with the four-vectors of both τ candidates (electrons, muons, or τ_h), resulting in an improved estimate of the four-vector of h boson that is then used to obtain a more accurate estimate of the A boson candidate mass $m_{\ell\ell\tau\tau}^{\text{fit}}$. The mass resolution of $m_{\ell\ell\tau\tau}^{\text{fit}}$ is 10% for an A boson with a mass of 300 GeV.

To further improve the mass resolution, the measured mass of the Higgs boson (125 GeV) can be given as an input to the SVFIT algorithm. This yields a constrained estimate of the four-vector of the h boson, which results in an even more precise estimate of the A boson candidate mass, denoted as $m_{\ell\ell\tau\tau}^{\text{c}}$. The resulting mass resolution of $m_{\ell\ell\tau\tau}^{\text{c}}$ is as good as 3% at 300 GeV, which improves the expected 95% confidence level (CL) model-independent limits by approximately 40% compared to using the visible mass of the A boson $m_{\ell\ell\tau\tau}^{\text{vis}}$ as the discriminating variable. Thus, we use $m_{\ell\ell\tau\tau}^{\text{c}}$ as the discriminating variable between the signal and the background processes for the final results.

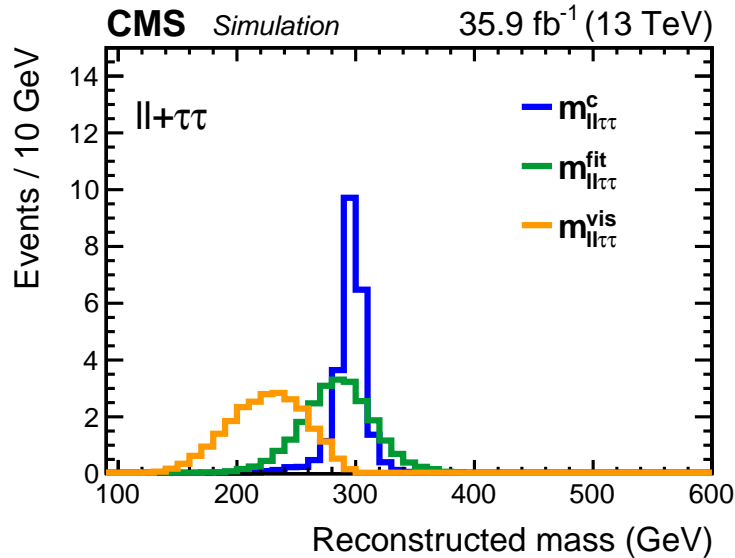


Figure 2: The distribution of the A boson mass for the three studied mass reconstruction methods at 300 GeV: using only the visible decay products ($m_{\ell\ell\tau\tau}^{\text{vis}}$, orange), using the SVFIT algorithm ($m_{\ell\ell\tau\tau}^{\text{fit}}$, green), and using the SVFIT algorithm with a mass constraint of 125 GeV for the Higgs boson ($m_{\ell\ell\tau\tau}^{\text{c}}$, blue). The eight final states of the A boson decay are combined for visualization purposes.

5 Event selection

Events are selected online using dilepton or single-lepton triggers targeting leptonic decays of the Z bosons. The trigger and offline selection requirements for the Z boson decay modes are presented in Table 1. Each lepton selected by the trigger is required to be geometrically matched to a corresponding lepton selected in the analysis. The light leptons in an event are required to be separated from each other by $\Delta R > 0.3$, while the τ_h candidates must be separated from each other and from any other lepton by $\Delta R > 0.5$. The resulting event samples are made mutually exclusive by discarding events that have additional identified and isolated electrons or muons. Small differences in trigger selection efficiencies are observed between data and simulation, and are accounted for by applying corrections to the simulated events.

The nontriggering electrons and muons are required to have $p_T > 10 \text{ GeV}$, whereas τ_h candidates are required to have $p_T > 20 \text{ GeV}$. The $|\eta|$ constraints from detector geometry are $|\eta^e| < 2.5$, $|\eta^\mu| < 2.4$, and $|\eta^{\tau_h}| < 2.3$ for electrons, muons, and τ_h candidates, respectively. The $|\eta|$ boundaries are the same for both triggering and nontriggering electrons and muons.

Table 1: Trigger and offline selection requirements for the different Z boson decay modes. The events are selected using either dilepton triggers with lower- p_T thresholds or single-lepton triggers with higher- p_T thresholds. The subscripts 1 and 2 indicate the higher- and lower- p_T leptons associated with the Z boson, respectively.

Decay channel	Z $\rightarrow \ell\ell$ trigger selection	Z $\rightarrow \ell\ell$ offline selection
Z $\rightarrow ee$	$[p_T^{e1} > 23 \text{ GeV} \ \& \ p_T^{e2} > 12 \text{ GeV}]$ or $p_T^{e1} > 27 \text{ GeV}$	$[p_T^{e1} > 24 \text{ GeV} \ \& \ p_T^{e2} > 13 \text{ GeV}]$ or $[p_T^{e1} > 28 \text{ GeV} \ \& \ p_T^{e2} > 10 \text{ GeV}]$
Z $\rightarrow \mu\mu$	$[p_T^{\mu1} > 17 \text{ GeV} \ \& \ p_T^{\mu2} > 8 \text{ GeV}]$ or $p_T^{\mu1} > 24 \text{ GeV}$	$[p_T^{\mu1} > 18 \text{ GeV} \ \& \ p_T^{\mu2} > 10 \text{ GeV}]$ or $[p_T^{\mu1} > 25 \text{ GeV} \ \& \ p_T^{\mu2} > 10 \text{ GeV}]$

The Z boson is reconstructed from a pair of opposite-charge, same-flavor light leptons that fulfills $60 < m_{\ell\ell} < 120 \text{ GeV}$. In case of multiple Z boson candidates, we choose the one with the mass closest to the Z boson mass. Loose identification and isolation selection criteria are applied to the leptons associated to the Z boson to maintain a high signal acceptance. The leptons forming the Z boson candidate are required to pass the lepton identification, which has an efficiency of 90 (>99)% for electrons (muons). The muons must pass an isolation requirement of $I^\mu < 0.25$, while a loose isolation requirement is already included in the electron identification selection.

The leptons associated with the h boson decay are required to have opposite charge. In case of the $e\tau_h$, $\mu\tau_h$, and $e\mu$ decay channels, tighter selection criteria are applied to the light leptons to decrease the background contributions from Z + jets and other reducible backgrounds. The specific signal selections detailed in Table 2, including those chosen for the τ_h candidates, were optimized to obtain the best signal sensitivity. The isolation requirements are $I^{e(\mu)} < 0.15$ for electrons (muons) associated to a tau lepton decay. Electrons from tau lepton decays need to pass the electron identification which has an efficiency of 80%. The τ_h candidates associated with the Higgs boson must satisfy the τ_h identification and isolation requirements which have an efficiency of 70%.

The large h boson mass leads to relatively high- p_T decay products compared to the lower p_T of jets misidentified as leptons from the Z + jets background process. This background process is suppressed by selecting events based on the scalar p_T sum of the visible decay products of the Higgs boson, L_T^h . In the $\ell\ell + \tau_h\tau_h$ final states, which have a larger relative ratio of reducible to

irreducible backgrounds, events with $L_T^h > 60$ GeV are selected.

The signal events contain no b jets ($gg \rightarrow A$), or only b jets with a relatively soft p_T distribution ($b\bar{b}A$). We suppress the contributions from background processes, especially $t\bar{t}$ and $t\bar{t}Z$, by discarding all events with one or more b-tagged jets with $p_T > 20$ GeV (“b jet veto”) without significantly reducing the signal selection efficiency. The total acceptance for the $gg \rightarrow A$ ($b\bar{b}A$) signal events with $m_A = 300$ GeV is 3.9 (3.0)%. The fraction of $gg \rightarrow A$ signal events lost due to the b jet veto is negligible, while for the $b\bar{b}A$ process approximately 17% of events are removed with this selection.

The sensitivity of the analysis is improved by reducing the number of background events using additional information regarding the Higgs boson candidate. The constrained Higgs boson candidate four-vector, as estimated with the SVFIT algorithm, is used to reconstruct the A boson mass, as described in Section 4. By removing the mass constraint from the SVFIT algorithm, the most likely mass of the Higgs boson candidate $m_{\tau\tau}^{\text{fit}}$ provides significant discrimination between reducible backgrounds, which have a broad distribution due to their nonresonant nature, and the signal processes, which have a resonance present at 125 GeV. Moreover, the dominant irreducible background from $ZZ \rightarrow 4\ell$ ($qq \rightarrow ZZ$ and $gg \rightarrow ZZ$) is suppressed, because for this background the $m_{\tau\tau}^{\text{fit}}$ distribution is concentrated near the Z boson mass in contrast to the signal. The signal sensitivity is increased by an additional 20% by requiring $m_{\tau\tau}^{\text{fit}}$ to be within 90–180 GeV.

Table 2: Kinematic selection requirements for each A boson decay channel, applied on top of the looser selections and b jet veto described in the text. The efficiency of the identification (and isolation) requirement for a given lepton type is labeled $\epsilon_{\text{id.}}^\ell$. The leptons assigned to the Higgs boson are required to have opposite charge. To increase the sensitivity, we require $m_{\tau\tau}^{\text{fit}}$ to be within 90–180 GeV. In the $\ell\ell + \tau_h\tau_h$ channel, we additionally require $L_T^h > 60$ GeV, where L_T^h is the scalar p_T sum of the visible decay products of the Higgs boson.

Channel	Z boson selection	h boson selection
$\ell\ell + e\tau_h$	$\left\{ \begin{array}{l} \text{Opposite-charge, same-flavor light leptons} \\ 60 < m_{\ell\ell} < 120 \text{ GeV} \end{array} \right\}$	$\epsilon_{\text{id.}}^e = 80\%, I^e < 0.15, \epsilon_{\text{id.+iso.}}^{\tau_h} = 70\%$
$\ell\ell + \mu\tau_h$		$\epsilon_{\text{id.}}^\mu > 99\%, I^\mu < 0.15, \epsilon_{\text{id.+iso.}}^{\tau_h} = 70\%$
$\ell\ell + \tau_h\tau_h$		$\epsilon_{\text{id.+iso.}}^{\tau_h} = 70\%, L_T^h > 60 \text{ GeV}$
$\ell\ell + e\mu$		$\epsilon_{\text{id.}}^e = 80\%, I^e < 0.15, \epsilon_{\text{id.}}^\mu > 99\%, I^\mu < 0.15$

6 Background estimation

The irreducible backgrounds ($ZZ \rightarrow 4\ell$, $t\bar{t}Z$, WWZ , WZZ , ZZZ) and the production of the 125 GeV Higgs boson via the processes predicted by the SM are estimated from simulation. They are scaled by their theoretical cross sections calculated at the highest order available, and the processes producing the 125 GeV Higgs boson are also scaled by their most accurate branching fractions [42].

The reducible backgrounds, which have at least one jet misidentified as an electron, muon, or τ_h candidate, are estimated from data. In this analysis the dominant reducible contributions come from the $t\bar{t}$, $Z + \text{jets}$, and $WZ + \text{jets}$ processes which produce jets misidentified as τ candidates. The estimation of the reducible background contribution is performed with a so-called “fake rate method” which is based on measuring the misidentification rates, i.e., probabilities to misidentify a jet as a lepton. Events with τ candidates failing the signal region identification and isolation criteria are used along with the misidentification rates to estimate the contribution from the reducible background in the signal region.

In total three different event samples are used to estimate the contribution from the reducible background processes. First, the misidentification rates are estimated in event samples independent from the signal region. This region is called a “measurement region”. To understand to which extent the measured misidentification rates describe the jets misidentified as leptons in the signal region, closure tests comparing the observed and the estimated reducible background yields are performed in yet another region (“validation region”). The validation region is required to be independent from the signal and the measurement regions. The closure tests are used to derive systematic uncertainties to account for possible differences between the true and the estimated reducible background yields in the signal region. Finally, the misidentification rates are applied in an “application region”, formed by events that fail the identification and isolation criteria required in the signal region.

In this analysis we use a sample of $Z + \text{jet}$ events to estimate the misidentification rates. The estimation of misidentification rates relies on reconstructing an opposite-charge, same-flavor lepton pair compatible with a Z boson, and requiring one additional loosely defined lepton (electron, muon, or τ_h candidate). The requirements on the leptons associated with the Z boson are the same as defined in Section 5, but they must fulfill a more stringent dilepton mass requirement, $81.2 < m_{\ell\ell} < 120 \text{ GeV}$. After reconstructing the $Z \rightarrow \ell\ell$ decay, the jet-to-lepton misidentification rate is estimated by applying the lepton identification algorithm to the additional loosely defined lepton in the event. The misidentification rates are measured in different bins of lepton p_T , and are further split between reconstructed decay modes for the τ_h candidate, and for muons and electrons in bins of lepton η , based on the barrel and endcap regions. The events where the τ candidates arise from genuine tau leptons, electrons, or muons and not jets, primarily from the WZ process, are estimated from simulation and subtracted from data so that the misidentification rates are measured for genuine hadronic jets only. The obtained misidentification rates for electrons (muons) are < 5 (10)% in barrel and endcap regions for lepton $p_T > 10 \text{ GeV}$, whereas for τ_h candidates the misidentification rates vary between 15–30% for τ_h candidate $p_T > 20 \text{ GeV}$ depending on the decay mode.

The measured misidentification rates are validated in another region that consists of events with a Z boson candidate and two additional loosely defined leptons. To ensure that the validation region is not contaminated with signal events or irreducible background contributions, the two additional leptons are required to have the same charge. Modest differences in observed versus predicted reducible background yields are observed. These differences are accounted for by assigning a systematic uncertainty in the yield, taken to be 40% which is conservative enough to cover the observed nonclosure. This uncertainty is uncorrelated between the Higgs boson decay channels resulting in four uncertainties tied to $\ell\ell + e\tau_h$, $\ell\ell + \mu\tau_h$, $\ell\ell + \tau_h\tau_h$, and $\ell\ell + e\mu$ channels. Further studies confirmed that the final results of this analysis are not sensitive to the exact magnitude of this systematic uncertainty.

To estimate the reducible background contribution in the signal region, we apply a weight on data events where either one or both of the τ candidates associated to the Higgs boson fail the identification and isolation criteria. These data events form the application region.

Events with exactly one object failing the identification and isolation criteria receive a weight $f/(1-f)$, where f is the misidentification rate for the particular type of lepton. As such, this weight includes the contribution from the $WZ + \text{jets}$ process, where we expect one genuine lepton and one jet misidentified as a lepton in addition to the Z boson candidate. Also $t\bar{t}$ and $Z + \text{jets}$ processes are accounted for by the weight as either of the two jets can pass the identification and isolation criteria even if neither of them is a genuine lepton. As a result, the weight introduces double counting of events from $t\bar{t}$ and $Z + \text{jets}$ processes.

To remove the double-counted events from $t\bar{t}$ and $Z + \text{jets}$ processes, we define a weight with a negative sign that is given for events with both objects failing the identification and isolation criteria, namely $-f_1 f_2 / [(1 - f_1)(1 - f_2)]$. This subtraction, however, introduces increased statistical uncertainties on the estimated yield of the reducible background.

The statistical uncertainties can be controlled by taking the shape of the $m_{\ell\ell\tau\tau}^c$ distribution of the reducible background contribution from data in another region with negligible signal and irreducible background contributions. This region is defined similarly to the signal region but with same-sign τ candidates passing relaxed identification and isolation criteria, yielding a higher number of events available for the shape estimation. This results in a smoother shape of the $m_{\ell\ell\tau\tau}^c$ distribution, which is normalized to the estimated yield of the reducible background contribution in the signal region.

An alternative approach to estimate the reducible background contribution was studied to reduce the statistical uncertainties and to cross check the results obtained using the nominal method. Instead of using the same-sign data events for the shape of the $m_{\ell\ell\tau\tau}^c$ distribution, the statistical uncertainties can be reduced considerably by giving a suitable nonzero weight only for events with both candidates failing the selection criteria, i.e., by estimating only the contribution from the $t\bar{t}$ and $Z + \text{jets}$ processes by using the misidentification rate method. The contribution from events with a single object failing the identification and isolation criteria is predicted from simulation, removing the double counting present in the nominal method. As a result, this alternative approach requires using a weight with a positive sign ($f_1 f_2 / [(1 - f_1)(1 - f_2)]$). Since the statistical uncertainties are smaller, the shape of the $m_{\ell\ell\tau\tau}^c$ distribution is taken from the same events that provide the estimated yield of the reducible background. The results of the cross-check show that the two methods yield consistent expected 95% CL model-independent limits.

To cross check the measured misidentification rates, we performed an additional measurement using a sample of $Z + 2 \text{ jets}$ events. In this cross-check, the measurement region partially overlaps with the aforementioned validation region, as in both cases the two lepton candidates are required to have the same charge. The amount of overlap between the measurement and validation regions depends on the lepton type and the decay channel of the Higgs boson. The rates are measured in bins of lepton p_T , and are separated by the reconstructed decay mode of the τ_h candidates. Unlike above, the misidentification rates are not split in bins of lepton η for electrons and muons. The measured misidentification rates result in a reducible background yield and shape that are compatible with the reducible background estimation obtained with the nominal misidentification rate measurement used in this analysis.

7 Systematic uncertainties

All systematic uncertainties considered in the analysis are summarized in Table 3. Different uncertainties are treated as uncorrelated, and each uncertainty is assumed correlated between different processes and final states, unless otherwise mentioned below.

The overall uncertainty in the τ_h identification and isolation efficiency for genuine τ_h leptons is 5% [93], which has been measured with a tag-and-probe method in $Z \rightarrow \tau\tau$ events. An uncertainty of 1.2% in the visible energy scale of genuine τ_h candidates affects both the distributions and yields of the signals and backgrounds. It is uncorrelated across the 1-prong, 1-prong+ π^0 s, and 3-prong decay modes.

The uncertainties in the electron and muon identification and isolation efficiencies lead to a

normalization uncertainty of 2% for either electrons or muons. The uncertainty in the trigger efficiency results in a normalization uncertainty of 2% for both electron and muon triggers. In all channels, the effect of the uncertainty in the electron and muon energy scales is negligible.

The normalization uncertainty related to vetoing events with a b-tagged jet is 4.5% for the background processes with heavy-flavor jets (from charm or bottom quarks), i.e., $t\bar{t}$, $t\bar{t}Z$, and $t\bar{t}W$. All other processes, including the signal process, are dominated by light-flavor or gluon jets and their normalization uncertainty is 0.15%.

The normalization uncertainties related to the choice of PDFs, and the renormalization and factorization (RF) scales, affecting the acceptance of the dominant background processes, are estimated from simulation separately for each process. The uncertainty from the RF scales is determined by varying one scale at a time by factors of 0.5 and 2.0, and calculating the change in process acceptance. Combining the RF scale uncertainties with the PDF set uncertainty [94] for the $qq \rightarrow ZZ$ process leads to an uncertainty of 4.8%. The inclusive uncertainty for Zh production related to the PDFs amounts to 1.6%, whereas the uncertainty for the variation of the RF scales is 3.8% [42]. For the subleading h boson processes Wh, $gg \rightarrow h \rightarrow ZZ$, and $t\bar{t}h$ the inclusive uncertainties related to the PDFs amount to 1.9, 3.2, and 3.6% and the uncertainties for the variation of the RF scales are 0.7, 3.9, and 7.5%, respectively [42].

For the $gg \rightarrow ZZ$ process, there is a 10% uncertainty in the NNLO cross section estimate used in the analysis, which covers the PDF, RF scale uncertainties, and the uncertainty on the strong coupling constant. An additional 10% uncertainty is included to account for the assumptions used to estimate the NNLO cross section [95]. The uncertainties in the cross section of the rare $t\bar{t}Z$, $t\bar{t}W$, and triboson processes amount to 25% [96].

The last theoretical uncertainty applied in this analysis is the uncertainty in the theoretical calculations of the SM $h \rightarrow \tau\tau$ branching fraction. This uncertainty of 2% [42] is applied to both the $gg \rightarrow A$ and $b\bar{b}A$ signal samples as well as all backgrounds that include the $h \rightarrow \tau\tau$ process.

Normalization uncertainties in the misidentification rates arising from the subtraction of prompt lepton contribution estimated from simulation are taken into account and propagated to the yield of the reducible background mass distributions. The shape of the $m_{\ell\ell\tau\tau}^c$ distribution of the reducible background is estimated from data in a region where the τ candidates have the same charge and pass relaxed isolation conditions. Therefore, the statistical uncertainties in the misidentification rates do not have an impact on the shape of the $m_{\ell\ell\tau\tau}^c$ distribution. As discussed in Section 6, an additional uncertainty is applied based on the results of the closure tests comparing the differences between the observed and the estimated reducible background yields. The uncertainty in the yield is taken to be 40%, and is considered uncorrelated across the $\ell\ell + e\tau_h$, $\ell\ell + \mu\tau_h$, $\ell\ell + \tau_h\tau_h$, and $\ell\ell + e\mu$ channels.

The \vec{p}_T^{miss} scale uncertainties [88], which are computed event-by-event, affect the normalization of various processes as well as their distributions through the propagation of these uncertainties to the di-tau masses $m_{\tau\tau}^{\text{fit}}$ and $m_{\tau\tau}^c$. The \vec{p}_T^{miss} scale uncertainties arising from unclustered energy deposits in the detector come from four independent sources related to the tracker, ECAL, hadron calorimeter, and forward calorimeters. The \vec{p}_T^{miss} scale uncertainties related to the uncertainties in the jet energy scale measurement, which affect the \vec{p}_T^{miss} calculation, are taken into account as a separate uncertainty.

Uncertainties related to the finite number of simulated events are taken into account using the Barlow-Beeston-lite method [97]. They are considered for all bins of the background distributions used to extract the results. They are uncorrelated across different samples,

and across bins of a single distribution. Finally, the uncertainty in the integrated luminosity amounts to 2.5% [98].

Table 3: Sources of systematic uncertainty. The sign † marks the uncertainties that affect both the shape and normalization of the final $m_{\ell\ell\tau\tau}^c$ distributions. Uncertainties that only affect the normalizations have no marker. For the shape and normalization uncertainties, the magnitude column lists an approximation of the associated change in the normalization of the affected processes.

Source of uncertainty	Process	Magnitude
τ_h id. & isolation	All simulated processes	5%
τ_h energy scale† (1.2% energy shift)	All simulated processes	<2%
e id. & isolation	All simulated processes	2%
e trigger	All simulated processes	2%
μ id. & isolation	All simulated processes	2%
μ trigger	All simulated processes	2%
b jet veto	All simulated processes	4.5% heavy flavor, 0.15% light flavor or gluon
qq \rightarrow ZZ theoretical uncertainty	qq \rightarrow ZZ	4.8%
PDF set uncertainty	Zh, Wh, gg \rightarrow h \rightarrow ZZ, and t \bar{t} h	Varies from 1.6 to 3.6% (see text)
RF scale uncertainty	Zh, Wh, gg \rightarrow h \rightarrow ZZ, and t \bar{t} h	Varies from 0.7 to 7.5% (see text)
gg \rightarrow ZZ theoretical uncertainty	gg \rightarrow ZZ	10%
gg \rightarrow ZZ NNLO cross section estimation assumptions	gg \rightarrow ZZ	10%
t \bar{t} Z theoretical uncertainty	t \bar{t} Z	25%
t \bar{t} W theoretical uncertainty	t \bar{t} W	25%
Triboson theoretical uncertainty	Triboson	25%
Theoretical uncertainty on $\mathcal{B}(h \rightarrow \tau\tau)$	Signal, Zh, and Wh	<2%
Reducible background uncertainties:	Reducible background	
e prompt lepton subtraction		<12% in $\ell\ell + e\mu$, <1% in $\ell\ell + e\tau_h$
μ prompt lepton subtraction		<16% in $\ell\ell + e\mu$, <1.5% in $\ell\ell + \mu\tau_h$
τ prompt lepton subtraction		<3.5% in $\ell\ell + e\tau_h$ and $\ell\ell + \mu\tau_{h'}$, <1% in $\ell\ell + \tau_h\tau_h$
Normalization		40% in $\ell\ell + e\tau_h$, $\ell\ell + \mu\tau_h$, $\ell\ell + \tau_h\tau_{h'}$, and $\ell\ell + e\mu$
\bar{p}_T^{miss} energy scale†	All simulated processes	<2%
Limited number of events	All background processes	Statistical uncertainty in individual bins
Integrated luminosity	All simulated processes	2.5%

8 Results

We use the reconstructed pseudoscalar Higgs boson mass, $m_{\ell\ell\tau\tau}^c$, as the discriminating variable between the signal and the background processes. The results are based on a simultaneous binned likelihood fit of the reconstructed mass distributions in the eight final states. The eight final states are each fit as separate distributions in the simultaneous fit. They are combined together for visualization purposes only. Nuisance parameters, representing the systematic uncertainties, are profiled in the fit. Even though the studied signal mass range is 220–400 GeV, the distribution of the reconstructed mass $m_{\ell\ell\tau\tau}^c$ covers the mass range 200–600 GeV, as the additional information on the background distributions is used to constrain the corresponding parameters in the simultaneous fit. When displaying the results, background processes are grouped as follows: “h(125 GeV)” includes all processes with the SM Higgs boson (including gg \rightarrow h \rightarrow ZZ \rightarrow 4 ℓ); “ZZ \rightarrow 4 ℓ ” includes events from qq \rightarrow ZZ and gg \rightarrow ZZ processes; “Other” includes events from triboson, t \bar{t} Z, and t \bar{t} W production; and “Reducible” includes the reducible background contribution.

The $m_{\ell\ell\tau\tau}^c$ distributions are shown in Fig. 3 for each of the four h boson decay channels, adding the Z \rightarrow $\ell\ell$ channels together, and in Fig. 4 for all eight final states together. The distributions are shown after a background-only fit to data and include both statistical and systematic uncertainties. No excess above the standard model background expectations is observed in data. The predicted signal and background yields, as well as the number of observed events, are given in Table 4 for each of the four Zh channels.

Upper limits at 95% CL [99, 100] are set in multiple scenarios. An asymptotic approximation of the modified frequentist CL_s method [99–102] is used when calculating the 95% CL upper

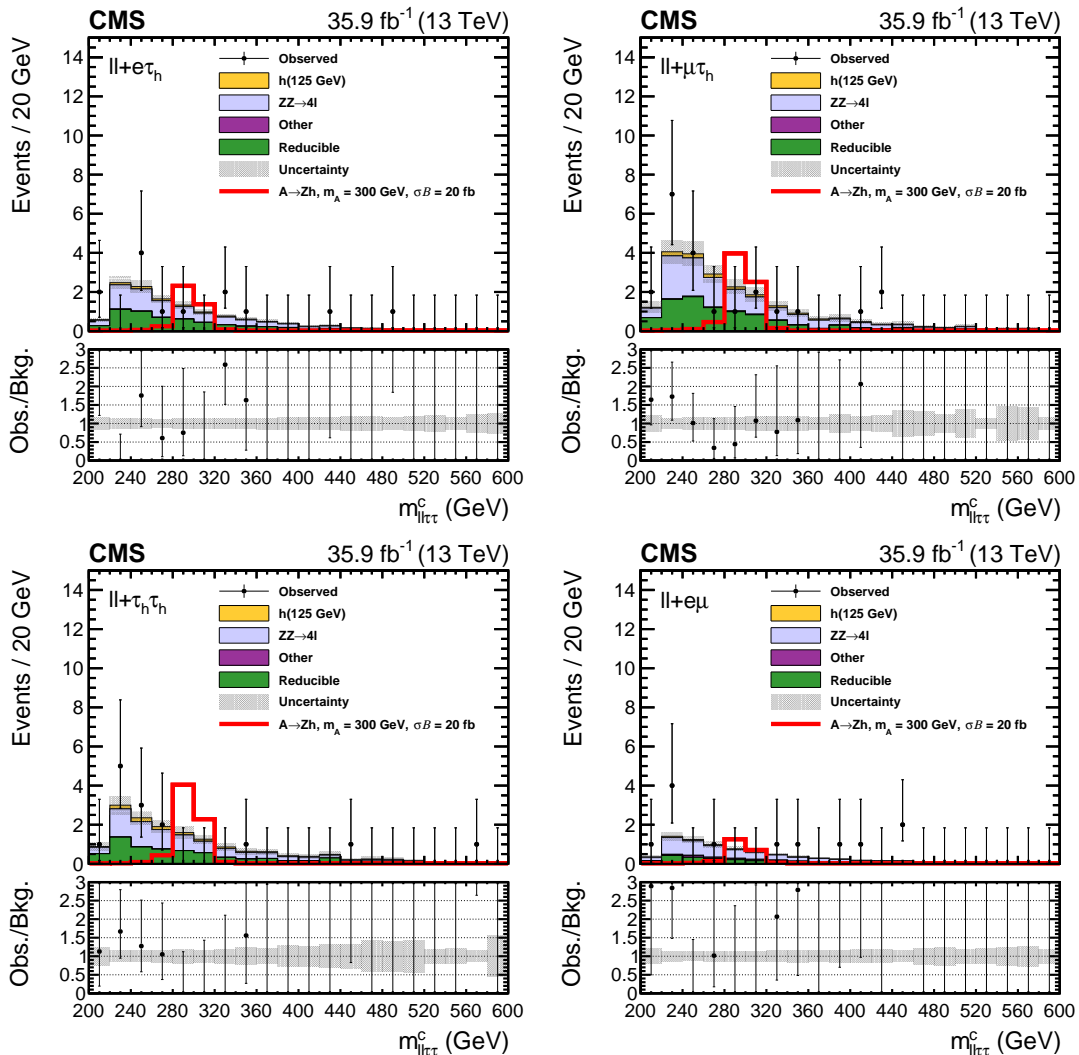


Figure 3: The reconstructed mass $m_{\ell\ell\tau\tau}^c$ distributions and uncertainties after a background-only fit for the $\ell\ell + e\tau_h$ (upper left), $\ell\ell + \mu\tau_h$ (upper right), $\ell\ell + \tau_h\tau_h$ (lower left), and $\ell\ell + e\mu$ (lower right) channels. In all cases the two decay channels of the Z boson are included as separate distributions in the simultaneous fit; combining them together is for visualization purposes only. The uncertainties include both statistical and systematic components. The expected contribution from the $A \rightarrow Zh$ signal process is shown for a pseudoscalar Higgs boson with $m_A = 300$ GeV with the product of the cross section and branching fraction of 20 fb and is for illustration only.

limits. Model-independent limits are set on the product of the cross section and branching fraction, $\sigma(gg \rightarrow A)\mathcal{B}(A \rightarrow Zh \rightarrow \ell\ell\tau\tau)$, for the $gg \rightarrow A \rightarrow Zh$ process. The model-independent 95% CL limits are shown in Fig. 5 and are consistent with the observed lack of signal.

Model-dependent interpretation of the results is performed in two MSSM scenarios, $M_{h,EFT}^{125}$ and hMSSM, setting 95% CL limits in the m_A - $\tan\beta$ plane. For both MSSM scenarios, limits are set based on the $gg \rightarrow A$ and $b\bar{b}A$ production processes. The signal samples used in the analysis are generated with the $gg \rightarrow A$ process. To account for the $b\bar{b}A$ production, at each point in the m_A - $\tan\beta$ plane, the yield of the signal process resulting from $gg \rightarrow A$ is scaled as

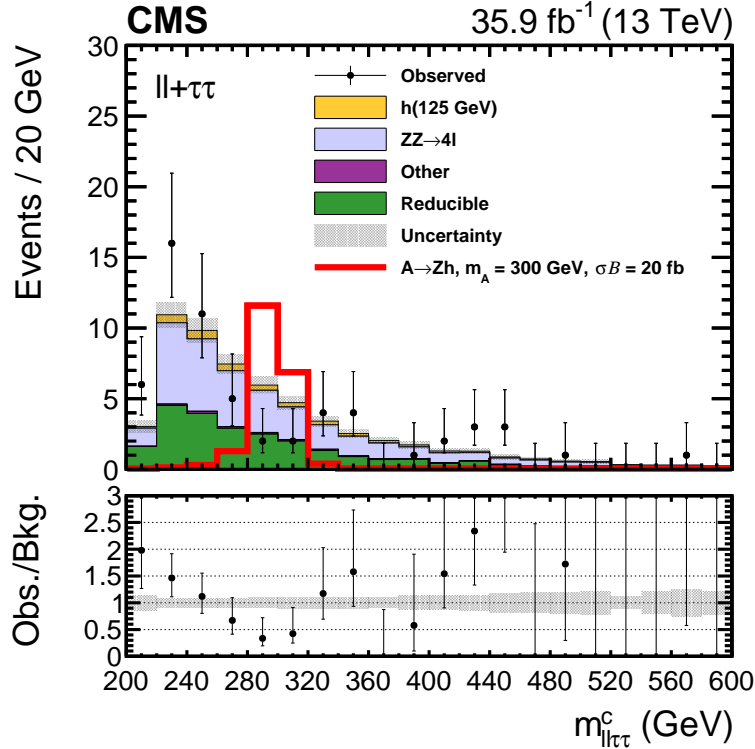


Figure 4: The reconstructed mass $m_{ll\tau\tau}^c$ distribution and uncertainties after a background-only fit in all eight final states. The final states are included as separate distributions in the simultaneous fit; combining them together is for visualization purposes only. The uncertainties include both statistical and systematic components. The expected contribution from the $A \rightarrow Zh$ signal process is shown for a pseudoscalar Higgs boson with $m_A = 300$ GeV with the product of the cross section and branching fraction of 20 fb and is for illustration only.

follows:

$$\text{Total signal yield} = gg \rightarrow A \text{ yield} \left(1 + \epsilon_{b\bar{b}A/gg \rightarrow A} \frac{\sigma_{b\bar{b}A}}{\sigma_{gg \rightarrow A}} \right). \quad (2)$$

The scaling takes the estimated $gg \rightarrow A$ yield at each m_A - $\tan \beta$ point and adds a contribution associated to $b\bar{b}A$ according to the estimated selection efficiency ratio in the signal region, $\epsilon_{b\bar{b}A/gg \rightarrow A} = 0.76$, and the ratio $\sigma_{b\bar{b}A}/\sigma_{gg \rightarrow A}$, which depends on m_A and $\tan \beta$. The signal region selection efficiency ratio was estimated for a single mass point ($m_A = 300$ GeV), and additional studies were performed to confirm that for the studied mass range (220–400 GeV) the efficiency ratio is nearly flat. The signal yield scaling allows the estimated $b\bar{b}A$ contribution to be included which is necessary when setting model-dependent limits in the parameter space region where the $b\bar{b}A$ cross section becomes nonnegligible compared to the $gg \rightarrow A$ cross section. For reference, at $m_A = 300$ GeV and $\tan \beta = 4$, in the hMSSM scenario, $\sigma_{b\bar{b}A}/\sigma_{gg \rightarrow A} = 0.22$, which is a nonnegligible contribution.

The results in the $M_{h,\text{EFT}}^{125}$ scenario and the hMSSM scenario are shown in Fig. 6. The observed limits exclude slightly higher $\tan \beta$ values in the $M_{h,\text{EFT}}^{125}$ scenario compared to the hMSSM scenario: for example at $m_A = 300$ GeV, $\tan \beta$ values below 4.0 and 3.7 are excluded at 95% confidence level in the $M_{h,\text{EFT}}^{125}$ and hMSSM scenarios, respectively.

In the hMSSM scenario, this search constrains the parameter space region with low $\tan \beta$ values when $220 < m_A < 350$ GeV, and supports the results of previous indirect and direct searches.

Table 4: Background and signal expectations together with the numbers of observed events, for the signal region distributions after a background-only fit. The expected contribution from the $A \rightarrow Zh$ signal process is given for a pseudoscalar Higgs boson with $m_A = 300$ GeV with the product of the cross section and branching fraction of 20 fb. The background uncertainty accounts for all sources of background uncertainty, systematic as well as statistical, after the simultaneous fit.

Process	$ll + e\tau_h$	$ll + \mu\tau_h$	$ll + \tau_h\tau_h$	$ll + e\mu$
h (125 GeV)	0.77 ± 0.02	1.39 ± 0.03	1.28 ± 0.04	0.45 ± 0.01
$ZZ \rightarrow 4\ell$	6.48 ± 0.13	11.38 ± 0.25	7.59 ± 0.20	4.57 ± 0.09
Other	0.10 ± 0.01	0.24 ± 0.02	0.04 ± 0.01	0.69 ± 0.04
Reducible	5.52 ± 0.42	9.12 ± 0.93	6.68 ± 0.65	2.04 ± 0.24
Total background	12.88 ± 0.45	22.13 ± 0.94	15.58 ± 0.68	7.74 ± 0.28
$A \rightarrow Zh, m_A = 300$ GeV, $\sigma\mathcal{B} = 20$ fb	4.13 ± 0.18	7.32 ± 0.30	7.01 ± 0.40	2.26 ± 0.10
Observed	13	22	14	12

The combined measurements of the standard model Higgs boson couplings result in indirect constraints on the hMSSM scenario, that indicate that m_A values below 600 GeV are disfavored by the observed data [16, 17]. Out of the direct searches targeting the m_A values below 400 GeV, this analysis has a similar sensitivity as the searches using the $A \rightarrow Zh(h \rightarrow b\bar{b})$ decay, performed by the ATLAS and CMS Collaborations [27, 28]. Moreover, together with the results presented in Refs. [27, 28], this analysis complements the constraints placed by analyses which target the decay of the H boson into a pair of W or Z bosons [103, 104].

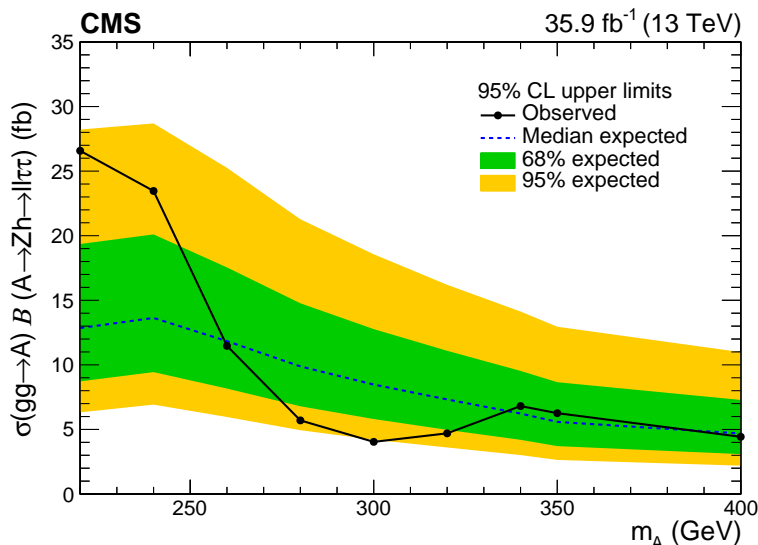


Figure 5: The expected and observed 95% CL model-independent upper limits on the product of the cross section and branching fraction $\sigma(gg \rightarrow A)\mathcal{B}(A \rightarrow Zh \rightarrow ll\tau\tau)$ are shown. The green (yellow) band corresponds to the 68 (95)% confidence intervals for the expected limit.

9 Summary

A search is presented for a pseudoscalar Higgs boson decaying into a 125 GeV Higgs boson, which further decays into tau leptons, and a Z boson that decays into a pair of electrons or muons. A data sample of proton-proton collisions collected at $\sqrt{s} = 13$ TeV by the CMS experiment at the LHC is used, corresponding to an integrated luminosity of 35.9 fb^{-1} . The

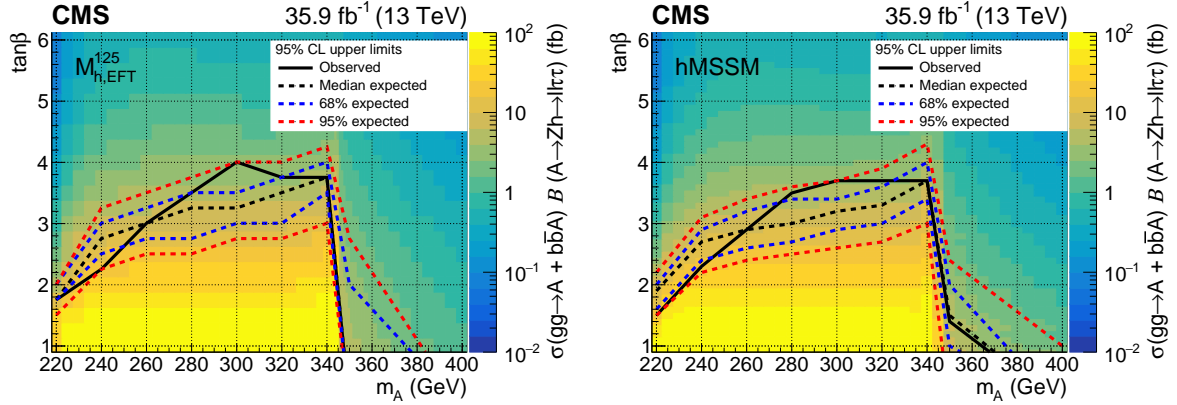


Figure 6: The expected and observed 95% CL exclusion limits in the m_A - $\tan\beta$ plane are shown for two MSSM scenarios: $M_{h,EFT}^{125}$ (left) and hMSSM (right). The area under the solid black curve is excluded. The dashed black curve corresponds to the median expected limit, surrounded by the 68 (95)% confidence intervals in blue (red). The limits are overlaid on a background showing the $\sigma(gg \rightarrow A + b\bar{b}A)\mathcal{B}(A \rightarrow Zh \rightarrow \ell\ell\tau\tau)$ as predicted by each model at each grid point.

sensitivity of the study is increased by using the information on the Higgs boson mass [13] when reconstructing the mass of the pseudoscalar Higgs boson. The signal extraction is further optimized with kinematic selections based on the mass of the Higgs boson. The data agree with the background predictions from the standard model. The observed model-independent limits at 95% confidence level on the product $\sigma(gg \rightarrow A)\mathcal{B}(A \rightarrow Zh \rightarrow \ell\ell\tau\tau)$ range from 27 to 5 fb for A boson mass 220 to 400 GeV, respectively. The model-independent limits are interpreted in terms of $\sigma(gg \rightarrow A + b\bar{b}A)\mathcal{B}(A \rightarrow Zh \rightarrow \ell\ell\tau\tau)$ for calculation of the model-dependent limits in two minimal supersymmetric standard model scenarios, $M_{h,EFT}^{125}$ and hMSSM. In the $M_{h,EFT}^{125}$ (hMSSM) scenario, the observed limits exclude $\tan\beta$ values below 1.8 (1.6) at $m_A = 220$ GeV and 4.0 (3.7) at $m_A = 300$ GeV at 95% confidence level.

Acknowledgments

We congratulate our colleagues in the CERN accelerator departments for the excellent performance of the LHC and thank the technical and administrative staffs at CERN and at other CMS institutes for their contributions to the success of the CMS effort. In addition, we gratefully acknowledge the computing centers and personnel of the Worldwide LHC Computing Grid for delivering so effectively the computing infrastructure essential to our analyses. Finally, we acknowledge the enduring support for the construction and operation of the LHC and the CMS detector provided by the following funding agencies: BMBWF and FWF (Austria); FNRS and FWO (Belgium); CNPq, CAPES, FAPERJ, FAPERGS, and FAPESP (Brazil); MES (Bulgaria); CERN; CAS, MoST, and NSFC (China); COLCIENCIAS (Colombia); MSES and CSF (Croatia); RPF (Cyprus); SENESCYT (Ecuador); MoER, ERC IUT, PUT and ERDF (Estonia); Academy of Finland, MEC, and HIP (Finland); CEA and CNRS/IN2P3 (France); BMBF, DFG, and HGF (Germany); GSRT (Greece); NKfIA (Hungary); DAE and DST (India); IPM (Iran); SFI (Ireland); INFN (Italy); MSIP and NRF (Republic of Korea); MES (Latvia); LAS (Lithuania); MOE and UM (Malaysia); BUAP, CINVESTAV, CONACYT, LNS, SEP, and UASLP-FAI (Mexico); MOS (Montenegro); MBIE (New Zealand); PAEC (Pakistan); MSHE and NSC (Poland); FCT (Portugal); JINR (Dubna); MON, RosAtom, RAS, RFBR, and NRC KI (Russia); MESTD (Serbia); SEIDI, CPAN, PCTI, and FEDER (Spain); MOSTR (Sri Lanka);

Swiss Funding Agencies (Switzerland); MST (Taipei); ThePCenter, IPST, STAR, and NSTDA (Thailand); TUBITAK and TAEK (Turkey); NASU (Ukraine); STFC (United Kingdom); DOE and NSF (USA).

Individuals have received support from the Marie-Curie program and the European Research Council and Horizon 2020 Grant, contract Nos. 675440, 752730, and 765710 (European Union); the Leventis Foundation; the A.P. Sloan Foundation; the Alexander von Humboldt Foundation; the Belgian Federal Science Policy Office; the Fonds pour la Formation à la Recherche dans l'Industrie et dans l'Agriculture (FRIA-Belgium); the Agentschap voor Innovatie door Wetenschap en Technologie (IWT-Belgium); the F.R.S.-FNRS and FWO (Belgium) under the "Excellence of Science – EOS" – be.h project n. 30820817; the Beijing Municipal Science & Technology Commission, No. Z181100004218003; the Ministry of Education, Youth and Sports (MEYS) of the Czech Republic; the Lendület ("Momentum") Program and the János Bolyai Research Scholarship of the Hungarian Academy of Sciences, the New National Excellence Program ÚNKP, the NKFI research grants 123842, 123959, 124845, 124850, 125105, 128713, 128786, and 129058 (Hungary); the Council of Science and Industrial Research, India; the HOMING PLUS program of the Foundation for Polish Science, cofinanced from European Union, Regional Development Fund, the Mobility Plus program of the Ministry of Science and Higher Education, the National Science Center (Poland), contracts Harmonia 2014/14/M/ST2/00428, Opus 2014/13/B/ST2/02543, 2014/15/B/ST2/03998, and 2015/19/B/ST2/02861, Sonata-bis 2012/07/E/ST2/01406; the National Priorities Research Program by Qatar National Research Fund; the Ministry of Science and Education, grant no. 3.2989.2017 (Russia); the Programa Estatal de Fomento de la Investigación Científica y Técnica de Excelencia María de Maeztu, grant MDM-2015-0509 and the Programa Severo Ochoa del Principado de Asturias; the Thalís and Aristeia programs cofinanced by EU-ESF and the Greek NSRF; the Rachadapisek Sompot Fund for Postdoctoral Fellowship, Chulalongkorn University and the Chulalongkorn Academic into Its 2nd Century Project Advancement Project (Thailand); the Nvidia Corporation; the Welch Foundation, contract C-1845; and the Weston Havens Foundation (USA).

References

- [1] S. L. Glashow, "Partial-symmetries of weak interactions", *Nuclear Physics* **22** (1961) 579, doi:10.1016/0029-5582(61)90469-2.
- [2] S. Weinberg, "A model of leptons", *Phys. Rev. Lett.* **19** (1967) 1264, doi:10.1103/PhysRevLett.19.1264.
- [3] A. Salam, "Weak and electromagnetic interactions", in *Elementary particle physics: relativistic groups and analyticity*, N. Svartholm, ed., p. 367. Almqvist & Wiksell, Stockholm, 1968. Proceedings of the eighth Nobel symposium.
- [4] F. Englert and R. Brout, "Broken symmetry and the mass of gauge vector mesons", *Phys. Rev. Lett.* **13** (1964) 321, doi:10.1103/PhysRevLett.13.321.
- [5] P. W. Higgs, "Broken symmetries, massless particles and gauge fields", *Phys. Lett.* **12** (1964) 132, doi:10.1016/0031-9163(64)91136-9.
- [6] P. W. Higgs, "Broken symmetries and the masses of gauge bosons", *Phys. Rev. Lett.* **13** (1964) 508, doi:10.1103/PhysRevLett.13.508.
- [7] G. S. Guralnik, C. R. Hagen, and T. W. B. Kibble, "Global conservation laws and massless particles", *Phys. Rev. Lett.* **13** (1964) 585, doi:10.1103/PhysRevLett.13.585.
- [8] P. W. Higgs, "Spontaneous symmetry breakdown without massless bosons", *Phys. Rev.* **145** (1966) 1156, doi:10.1103/PhysRev.145.1156.
- [9] T. W. B. Kibble, "Symmetry breaking in non-Abelian gauge theories", *Phys. Rev.* **155** (1967) 1554, doi:10.1103/PhysRev.155.1554.
- [10] ATLAS Collaboration, "Observation of a new particle in the search for the standard model Higgs boson with the ATLAS detector at the LHC", *Phys. Lett. B* **716** (2012) 1, doi:10.1016/j.physletb.2012.08.020, arXiv:1207.7214.
- [11] CMS Collaboration, "Observation of a new boson at a mass of 125 GeV with the CMS experiment at the LHC", *Phys. Lett. B* **716** (2012) 30, doi:10.1016/j.physletb.2012.08.021, arXiv:1207.7235.
- [12] CMS Collaboration, "Observation of a new boson with mass near 125 GeV in pp collisions at $\sqrt{s} = 7$ and 8 TeV", *JHEP* **06** (2013) 081, doi:10.1007/JHEP06(2013)081, arXiv:1303.4571.
- [13] CMS Collaboration, "Measurements of properties of the Higgs boson decaying into the four-lepton final state in pp collisions at $\sqrt{s} = 13$ TeV", *JHEP* **11** (2017) 047, doi:10.1007/JHEP11(2017)047, arXiv:1706.09936.
- [14] ATLAS and CMS Collaborations, "Combined measurement of the Higgs boson mass in pp collisions at $\sqrt{s} = 7$ and 8 TeV with the ATLAS and CMS experiments", *Phys. Rev. Lett.* **114** (2015) 191803, doi:10.1103/PhysRevLett.114.191803, arXiv:1503.07589.
- [15] ATLAS Collaboration, "Measurement of the Higgs boson mass in the $H \rightarrow ZZ^* \rightarrow 4\ell$ and $H \rightarrow \gamma\gamma$ channels with $\sqrt{s} = 13$ TeV pp collisions using the ATLAS detector", *Phys. Lett. B* **784** (2018) 345, doi:10.1016/j.physletb.2018.07.050, arXiv:1806.00242.

- [16] ATLAS Collaboration, “Combined measurements of Higgs boson production and decay using up to 80 fb^{-1} of proton-proton collision data at $\sqrt{s} = 13 \text{ TeV}$ collected with the ATLAS experiment”, *Phys. Rev. D* **101** (2020) 012002, doi:10.1103/PhysRevD.101.012002, arXiv:1909.02845.
- [17] CMS Collaboration, “Combined measurements of Higgs boson couplings in proton-proton collisions at $\sqrt{s} = 13 \text{ TeV}$ ”, *Eur. Phys. J. C* **79** (2019) 421, doi:10.1140/epjc/s10052-019-6909-y, arXiv:1809.10733.
- [18] T. D. Lee, “A theory of spontaneous T violation”, *Phys. Rev. D* **8** (1973) 1226, doi:10.1103/PhysRevD.8.1226.
- [19] G. C. Branco et al., “Theory and phenomenology of two-Higgs-doublet models”, *Phys. Rept.* **516** (2012) 1, doi:10.1016/j.physrep.2012.02.002, arXiv:1106.0034.
- [20] H. Bahl, S. Liebler, and T. Stefaniak, “MSSM Higgs benchmark scenarios for Run 2 and beyond: the low $\tan\beta$ region”, *Eur. Phys. J. C* **79** (2019) 279, doi:10.1140/epjc/s10052-019-6770-z, arXiv:1901.05933.
- [21] A. Djouadi and J. Quevillon, “The MSSM Higgs sector at a high M_{SUSY} : reopening the low $\tan\beta$ regime and heavy Higgs searches”, *JHEP* **10** (2013) 028, doi:10.1007/JHEP10(2013)028, arXiv:1304.1787.
- [22] L. Maiani, A. D. Polosa, and V. Riquer, “Bounds to the Higgs sector masses in minimal supersymmetry from LHC data”, *Phys. Lett. B* **724** (2013) 274, doi:10.1016/j.physletb.2013.06.026, arXiv:1305.2172.
- [23] A. Djouadi et al., “The post-Higgs MSSM scenario: Habemus MSSM?”, *Eur. Phys. J. C* **73** (2013) 2650, doi:10.1140/epjc/s10052-013-2650-0, arXiv:1307.5205.
- [24] A. Djouadi et al., “Fully covering the MSSM Higgs sector at the LHC”, *JHEP* **06** (2015) 168, doi:10.1007/JHEP06(2015)168, arXiv:1502.05653.
- [25] ATLAS Collaboration, “Search for a CP-odd Higgs boson decaying to Zh in pp collisions at $\sqrt{s} = 8 \text{ TeV}$ with the ATLAS detector”, *Phys. Lett. B* **744** (2015) 163, doi:10.1016/j.physletb.2015.03.054, arXiv:1502.04478.
- [26] CMS Collaboration, “Searches for a heavy scalar boson H decaying to a pair of 125 GeV Higgs bosons hh or for a heavy pseudoscalar boson A decaying to Zh , in the final states with $h \rightarrow \tau\tau$ ”, *Phys. Lett. B* **755** (2016) 217, doi:10.1016/j.physletb.2016.01.056, arXiv:1510.01181.
- [27] ATLAS Collaboration, “Search for heavy resonances decaying into a W or Z boson and a Higgs boson in final states with leptons and b -jets in 36 fb^{-1} of $\sqrt{s} = 13 \text{ TeV}$ pp collisions with the ATLAS detector”, *JHEP* **03** (2018) 174, doi:10.1007/JHEP03(2018)174, arXiv:1712.06518. [Erratum: doi:10.1007/JHEP11(2018)051].
- [28] CMS Collaboration, “Search for a heavy pseudoscalar boson decaying to a Z and a Higgs boson at $\sqrt{s} = 13 \text{ TeV}$ ”, *Eur. Phys. J. C* **79** (2019) 564, doi:10.1140/epjc/s10052-019-7058-z, arXiv:1903.00941.
- [29] L. Bianchini et al., “Reconstruction of the Higgs mass in events with Higgs bosons decaying into a pair of τ leptons using matrix element techniques”, *Nucl. Instrum. Meth. A* **862** (2017) 54, doi:10.1016/j.nima.2017.05.001, arXiv:1603.05910.

-
- [30] CMS Collaboration, “The CMS trigger system”, *JINST* **12** (2017) P01020, doi:10.1088/1748-0221/12/01/P01020, arXiv:1609.02366.
- [31] CMS Collaboration, “The CMS experiment at the CERN LHC”, *JINST* **3** (2008) S08004, doi:10.1088/1748-0221/3/08/S08004.
- [32] J. Alwall et al., “The automated computation of tree-level and next-to-leading order differential cross sections, and their matching to parton shower simulations”, *JHEP* **07** (2014) 079, doi:10.1007/JHEP07(2014)079, arXiv:1405.0301.
- [33] M. Carena et al., “MSSM Higgs boson searches at the LHC: Benchmark scenarios after the discovery of a Higgs-like particle”, *Eur. Phys. J. C* **73** (2013) 2552, doi:10.1140/epjc/s10052-013-2552-1, arXiv:1302.7033.
- [34] P. Nason, “A new method for combining NLO QCD with shower Monte Carlo algorithms”, *JHEP* **11** (2004) 040, doi:10.1088/1126-6708/2004/11/040, arXiv:hep-ph/0409146.
- [35] S. Frixione, P. Nason, and C. Oleari, “Matching NLO QCD computations with parton shower simulations: the POWHEG method”, *JHEP* **11** (2007) 070, doi:10.1088/1126-6708/2007/11/070, arXiv:0709.2092.
- [36] S. Alioli, P. Nason, C. Oleari, and E. Re, “A general framework for implementing NLO calculations in shower Monte Carlo programs: the POWHEG BOX”, *JHEP* **06** (2010) 043, doi:10.1007/JHEP06(2010)043, arXiv:1002.2581.
- [37] S. Alioli et al., “Jet pair production in POWHEG”, *JHEP* **04** (2011) 081, doi:10.1007/JHEP04(2011)081, arXiv:1012.3380.
- [38] S. Alioli, P. Nason, C. Oleari, and E. Re, “NLO Higgs boson production via gluon fusion matched with shower in POWHEG”, *JHEP* **04** (2009) 002, doi:10.1088/1126-6708/2009/04/002, arXiv:0812.0578.
- [39] G. Luisoni, P. Nason, C. Oleari, and F. Tramontano, “ $HW^\pm/HZ + 0$ and 1 jet at NLO with the POWHEG BOX interfaced to GoSam and their merging within MiNLO”, *JHEP* **10** (2013) 083, doi:10.1007/JHEP10(2013)083, arXiv:1306.2542.
- [40] D. de Florian, G. Ferrera, M. Grazzini, and D. Tommasini, “Higgs boson production at the LHC: Transverse momentum resummation effects in the $H \rightarrow \gamma\gamma$, $H \rightarrow WW \rightarrow l\nu l\nu$ and $H \rightarrow ZZ \rightarrow 4l$ decay modes”, *JHEP* **06** (2012) 132, doi:10.1007/JHEP06(2012)132, arXiv:1203.6321.
- [41] M. Grazzini and H. Sargsyan, “Heavy-quark mass effects in Higgs boson production at the LHC”, *JHEP* **09** (2013) 129, doi:10.1007/JHEP09(2013)129, arXiv:1306.4581.
- [42] LHC Higgs Cross Section Working Group, “Handbook of LHC Higgs cross sections: 4. Deciphering the nature of the Higgs sector”, (2016). arXiv:1610.07922.
- [43] A. Denner et al., “Standard model Higgs-boson branching ratios with uncertainties”, *Eur. Phys. J. C* **71** (2011) 1753, doi:10.1140/epjc/s10052-011-1753-8, arXiv:1107.5909.

- [44] NNPDF Collaboration, “Impact of heavy quark masses on parton distributions and LHC phenomenology”, *Nucl. Phys. B* **849** (2011) 296, doi:10.1016/j.nuclphysb.2011.03.021, arXiv:1101.1300.
- [45] J. M. Campbell and R. K. Ellis, “MCFM for the Tevatron and the LHC”, *Nucl. Phys. B Proc. Suppl.* **205-206** (2010) 10, doi:10.1016/j.nuclphysbps.2010.08.011, arXiv:1007.3492.
- [46] R. Frederix and S. Frixione, “Merging meets matching in MC@NLO”, *JHEP* **12** (2012) 061, doi:10.1007/JHEP12(2012)061, arXiv:1209.6215.
- [47] J. Alwall et al., “Comparative study of various algorithms for the merging of parton showers and matrix elements in hadronic collisions”, *Eur. Phys. J. C* **53** (2008) 473, doi:10.1140/epjc/s10052-007-0490-5, arXiv:0706.2569.
- [48] T. Sjöstrand et al., “An introduction to PYTHIA 8.2”, *Comput. Phys. Commun.* **191** (2015) 159, doi:10.1016/j.cpc.2015.01.024, arXiv:1410.3012.
- [49] CMS Collaboration, “Event generator tunes obtained from underlying event and multiparton scattering measurements”, *Eur. Phys. J. C* **76** (2016) 155, doi:10.1140/epjc/s10052-016-3988-x, arXiv:1512.00815.
- [50] R. D. Ball et al., “Unbiased global determination of parton distributions and their uncertainties at NNLO and at LO”, *Nucl. Phys. B* **855** (2012) 153, doi:10.1016/j.nuclphysb.2011.09.024, arXiv:1107.2652.
- [51] GEANT4 Collaboration, “GEANT4—a simulation toolkit”, *Nucl. Instrum. Meth. A* **506** (2003) 250, doi:10.1016/S0168-9002(03)01368-8.
- [52] S. Heinemeyer, W. Hollik, and G. Weiglein, “FeynHiggs: A program for the calculation of the masses of the neutral CP-even Higgs bosons in the MSSM”, *Comput. Phys. Commun.* **124** (2000) 76, doi:10.1016/S0010-4655(99)00364-1, arXiv:hep-ph/9812320.
- [53] S. Heinemeyer, W. Hollik, and G. Weiglein, “The masses of the neutral CP-even Higgs bosons in the MSSM: Accurate analysis at the two-loop level”, *Eur. Phys. J. C* **9** (1999) 343, doi:10.1007/s100529900006, arXiv:hep-ph/9812472.
- [54] G. Degross et al., “Towards high-precision predictions for the MSSM Higgs sector”, *Eur. Phys. J. C* **28** (2003) 133, doi:10.1140/epjc/s2003-01152-2, arXiv:hep-ph/0212020.
- [55] M. Frank et al., “The Higgs boson masses and mixings of the complex MSSM in the Feynman-diagrammatic approach”, *JHEP* **02** (2007) 047, doi:10.1088/1126-6708/2007/02/047, arXiv:hep-ph/0611326.
- [56] T. Hahn et al., “High-precision predictions for the light CP-even Higgs boson mass of the minimal supersymmetric standard model”, *Phys. Rev. Lett.* **112** (2014) 141801, doi:10.1103/PhysRevLett.112.141801, arXiv:1312.4937.
- [57] R. V. Harlander, S. Liebler, and H. Mantler, “SusHi: A program for the calculation of Higgs production in gluon fusion and bottom-quark annihilation in the standard model and the MSSM”, *Comput. Phys. Commun.* **184** (2013) 1605, doi:10.1016/j.cpc.2013.02.006, arXiv:1212.3249.

-
- [58] R. V. Harlander, S. Liebler, and H. Mantler, “SusHi Bento: Beyond NNLO and the heavy-top limit”, *Comput. Phys. Commun.* **212** (2017) 239, doi:10.1016/j.cpc.2016.10.015, arXiv:1605.03190.
- [59] M. Spira, A. Djouadi, D. Graudenz, and P. M. Zerwas, “Higgs boson production at the LHC”, *Nucl. Phys. B* **453** (1995) 17, doi:10.1016/0550-3213(95)00379-7, arXiv:hep-ph/9504378.
- [60] R. V. Harlander and M. Steinhauser, “Supersymmetric Higgs production in gluon fusion at next-to-leading order”, *JHEP* **09** (2004) 066, doi:10.1088/1126-6708/2004/09/066, arXiv:hep-ph/0409010.
- [61] R. Harlander and P. Kant, “Higgs production and decay: Analytic results at next-to-leading order QCD”, *JHEP* **12** (2005) 015, doi:10.1088/1126-6708/2005/12/015, arXiv:hep-ph/0509189.
- [62] G. Degrandi and P. Slavich, “NLO QCD bottom corrections to Higgs boson production in the MSSM”, *JHEP* **11** (2010) 044, doi:10.1007/JHEP11(2010)044, arXiv:1007.3465.
- [63] G. Degrandi, S. Di Vita, and P. Slavich, “NLO QCD corrections to pseudoscalar Higgs production in the MSSM”, *JHEP* **08** (2011) 128, doi:10.1007/JHEP08(2011)128, arXiv:1107.0914.
- [64] G. Degrandi, S. Di Vita, and P. Slavich, “On the NLO QCD corrections to the production of the heaviest neutral Higgs scalar in the MSSM”, *Eur. Phys. J. C* **72** (2012) 2032, doi:10.1140/epjc/s10052-012-2032-z, arXiv:1204.1016.
- [65] R. V. Harlander and W. B. Kilgore, “Next-to-next-to-leading order Higgs production at hadron colliders”, *Phys. Rev. Lett.* **88** (2002) 201801, doi:10.1103/PhysRevLett.88.201801, arXiv:hep-ph/0201206.
- [66] C. Anastasiou and K. Melnikov, “Higgs boson production at hadron colliders in NNLO QCD”, *Nucl. Phys. B* **646** (2002) 220, doi:10.1016/S0550-3213(02)00837-4, arXiv:hep-ph/0207004.
- [67] V. Ravindran, J. Smith, and W. L. van Neerven, “NNLO corrections to the total cross-section for Higgs boson production in hadron-hadron collisions”, *Nucl. Phys. B* **665** (2003) 325, doi:10.1016/S0550-3213(03)00457-7, arXiv:hep-ph/0302135.
- [68] R. V. Harlander and W. B. Kilgore, “Production of a pseudo-scalar Higgs boson at hadron colliders at next-to-next-to leading order”, *JHEP* **10** (2002) 017, doi:10.1088/1126-6708/2002/10/017, arXiv:hep-ph/0208096.
- [69] C. Anastasiou and K. Melnikov, “Pseudoscalar Higgs boson production at hadron colliders in next-to-next-to-leading order QCD”, *Phys. Rev. D* **67** (2003) 037501, doi:10.1103/PhysRevD.67.037501, arXiv:hep-ph/0208115.
- [70] U. Aglietti, R. Bonciani, G. Degrandi, and A. Vicini, “Two-loop light fermion contribution to Higgs production and decays”, *Phys. Lett. B* **595** (2004) 432, doi:10.1016/j.physletb.2004.06.063, arXiv:hep-ph/0404071.

- [71] R. Bonciani, G. Degrossi, and A. Vicini, "On the generalized harmonic polylogarithms of one complex variable", *Comput. Phys. Commun.* **182** (2011) 1253, doi:10.1016/j.cpc.2011.02.011, arXiv:1007.1891.
- [72] R. V. Harlander and W. B. Kilgore, "Higgs boson production in bottom quark fusion at next-to-next-to leading order", *Phys. Rev. D* **68** (2003) 013001, doi:10.1103/PhysRevD.68.013001, arXiv:hep-ph/0304035.
- [73] S. Dittmaier, M. Krämer, and M. Spira, "Higgs radiation off bottom quarks at the Fermilab Tevatron and the CERN LHC", *Phys. Rev. D* **70** (2004) 074010, doi:10.1103/PhysRevD.70.074010, arXiv:hep-ph/0309204.
- [74] S. Dawson, C. B. Jackson, L. Reina, and D. Wackerroth, "Exclusive Higgs boson production with bottom quarks at hadron colliders", *Phys. Rev. D* **69** (2004) 074027, doi:10.1103/PhysRevD.69.074027, arXiv:hep-ph/0311067.
- [75] R. Harlander, M. Kramer, and M. Schumacher, "Bottom-quark associated Higgs-boson production: reconciling the four- and five-flavour scheme approach", (2011). arXiv:1112.3478.
- [76] M. Bonvini, A. S. Papanastasiou, and F. J. Tackmann, "Resummation and matching of b-quark mass effects in $b\bar{b}H$ production", *JHEP* **11** (2015) 196, doi:10.1007/JHEP11(2015)196, arXiv:1508.03288.
- [77] M. Bonvini, A. S. Papanastasiou, and F. J. Tackmann, "Matched predictions for the $b\bar{b}H$ cross section at the 13 TeV LHC", *JHEP* **10** (2016) 053, doi:10.1007/JHEP10(2016)053, arXiv:1605.01733.
- [78] S. Forte, D. Napoletano, and M. Ubiali, "Higgs production in bottom-quark fusion in a matched scheme", *Phys. Lett. B* **751** (2015) 331, doi:10.1016/j.physletb.2015.10.051, arXiv:1508.01529.
- [79] S. Forte, D. Napoletano, and M. Ubiali, "Higgs production in bottom-quark fusion: matching beyond leading order", *Phys. Lett. B* **763** (2016) 190, doi:10.1016/j.physletb.2016.10.040, arXiv:1607.00389.
- [80] A. Djouadi, J. Kalinowski, and M. Spira, "HDECAY: A program for Higgs boson decays in the standard model and its supersymmetric extension", *Comput. Phys. Commun.* **108** (1998) 56, doi:10.1016/S0010-4655(97)00123-9, arXiv:hep-ph/9704448.
- [81] A. Djouadi, M. M. Mühlleitner, and M. Spira, "Decays of supersymmetric particles: The program SUSY-HIT (SUSpect-SdecaY-Hdecay-InTerface)", in *Physics at LHC. Proceedings, 3rd Conference*, p. 635. Cracow, Poland, July, 2006. arXiv:hep-ph/0609292. [*Acta Phys. Polon. B* 38 (2007) 38].
- [82] A. Djouadi, J. Kalinowski, M. Mühlleitner, and M. Spira, "HDECAY: Twenty₊₊ years after", *Comput. Phys. Commun.* **238** (2019) 214, doi:10.1016/j.cpc.2018.12.010, arXiv:1801.09506.
- [83] CMS Collaboration, "Particle-flow reconstruction and global event description with the CMS detector", *JINST* **12** (2017) P10003, doi:10.1088/1748-0221/12/10/P10003, arXiv:1706.04965.
- [84] M. Cacciari, G. P. Salam, and G. Soyez, "FastJet user manual", *Eur. Phys. J. C* **72** (2012) 1896, doi:10.1140/epjc/s10052-012-1896-2, arXiv:1111.6097.

-
- [85] M. Cacciari and G. P. Salam, “Dispelling the N^3 myth for the k_T jet-finder”, *Phys. Lett. B* **641** (2006) 57, doi:10.1016/j.physletb.2006.08.037, arXiv:hep-ph/0512210.
- [86] M. Cacciari, G. P. Salam, and G. Soyez, “The anti- k_T jet clustering algorithm”, *JHEP* **04** (2008) 063, doi:10.1088/1126-6708/2008/04/063, arXiv:0802.1189.
- [87] CMS Collaboration, “Jet energy scale and resolution in the CMS experiment in pp collisions at 8 TeV”, *JINST* **12** (2017) P02014, doi:10.1088/1748-0221/12/02/P02014, arXiv:1607.03663.
- [88] CMS Collaboration, “Performance of missing transverse momentum reconstruction in proton-proton collisions at $\sqrt{s} = 13$ TeV using the CMS detector”, *JINST* **14** (2019) P07004, doi:10.1088/1748-0221/14/07/P07004, arXiv:1903.06078.
- [89] CMS Collaboration, “Performance of electron reconstruction and selection with the CMS detector in proton-proton collisions at $\sqrt{s} = 8$ TeV”, *JINST* **10** (2015) P06005, doi:10.1088/1748-0221/10/06/P06005, arXiv:1502.02701.
- [90] CMS Collaboration, “Performance of the CMS muon detector and muon reconstruction with proton-proton collisions at $\sqrt{s} = 13$ TeV”, *JINST* **13** (2018) P06015, doi:10.1088/1748-0221/13/06/P06015, arXiv:1804.04528.
- [91] CMS Collaboration, “Identification of heavy-flavour jets with the CMS detector in pp collisions at 13 TeV”, *JINST* **13** (2017) P05011, doi:10.1088/1748-0221/13/05/P05011, arXiv:1712.07158.
- [92] CMS Collaboration, “Reconstruction and identification of τ lepton decays to hadrons and ν_τ at CMS”, *JINST* **11** (2016) P01019, doi:10.1088/1748-0221/11/01/P01019, arXiv:1510.07488.
- [93] CMS Collaboration, “Performance of reconstruction and identification of τ leptons decaying to hadrons and ν_τ in pp collisions at $\sqrt{s} = 13$ TeV”, *JINST* **13** (2018) P10005, doi:10.1088/1748-0221/13/10/P10005, arXiv:1809.02816.
- [94] J. Butterworth et al., “PDF4LHC recommendations for LHC Run II”, *J. Phys. G* **43** (2016) 023001, doi:10.1088/0954-3899/43/2/023001, arXiv:1510.03865.
- [95] CMS Collaboration, “Measurements of the Higgs boson width and anomalous HVV couplings from on-shell and off-shell production in the four-lepton final state”, *Phys. Rev. D* **99** (2019) 112003, doi:10.1103/PhysRevD.99.112003, arXiv:1901.00174.
- [96] CMS Collaboration, “Measurement of the cross section for top quark pair production in association with a W or Z boson in proton-proton collisions at $\sqrt{s} = 13$ TeV”, *JHEP* **08** (2018) 011, doi:10.1007/JHEP08(2018)011, arXiv:1711.02547.
- [97] R. J. Barlow and C. Beeston, “Fitting using finite Monte Carlo samples”, *Comput. Phys. Commun.* **77** (1993) 219, doi:10.1016/0010-4655(93)90005-w.
- [98] CMS Collaboration, “CMS luminosity measurements for the 2016 data taking period”, CMS Physics Analysis Summary CMS-PAS-LUM-17-001, 2017.

- [99] T. Junk, "Confidence level computation for combining searches with small statistics", *Nucl. Instrum. Meth. A* **434** (1999) 435, doi:10.1016/S0168-9002(99)00498-2, arXiv:hep-ex/9902006.
- [100] A. L. Read, "Presentation of search results: The CL_s technique", *J. Phys. G* **28** (2002) 2693, doi:10.1088/0954-3899/28/10/313.
- [101] ATLAS and CMS Collaborations, The LHC Higgs Combination Group, "Procedure for the LHC Higgs boson search combination in Summer 2011", Technical Report CMS-NOTE-2011-005. ATL-PHYS-PUB-2011-11, 2011.
- [102] G. Cowan, K. Cranmer, E. Gross, and O. Vitells, "Asymptotic formulae for likelihood-based tests of new physics", *Eur. Phys. J. C* **71** (2011) 1554, doi:10.1140/epjc/s10052-011-1554-0, arXiv:1007.1727. [Erratum: doi:10.1140/epjc/s10052-013-2501-z].
- [103] ATLAS Collaboration, "Search for heavy resonances decaying into WW in the $e\nu\mu\nu$ final state in pp collisions at $\sqrt{s} = 13$ TeV with the ATLAS detector", *Eur. Phys. J. C* **78** (2018) 24, doi:10.1140/epjc/s10052-017-5491-4, arXiv:1710.01123.
- [104] ATLAS Collaboration, "Search for heavy ZZ resonances in the $\ell^+\ell^-\ell^+\ell^-$ and $\ell^+\ell^-\nu\bar{\nu}$ final states using proton proton collisions at $\sqrt{s} = 13$ TeV with the ATLAS detector. Search for heavy ZZ resonances in the $\ell^+\ell^-\ell^+\ell^-$ and $\ell^+\ell^-\nu\bar{\nu}$ final states using proton proton collisions at $\sqrt{s} = 13$ TeV with the ATLAS detector", *Eur. Phys. J. C* **78** (2018) 293, doi:10.1140/epjc/s10052-018-5686-3, arXiv:1712.06386.

A The CMS Collaboration

Yerevan Physics Institute, Yerevan, Armenia

A.M. Sirunyan[†], A. Tumasyan

Institut für Hochenergiephysik, Wien, Austria

W. Adam, F. Ambrogio, T. Bergauer, J. Brandstetter, M. Dragicevic, J. Erö, A. Escalante Del Valle, M. Flechl, R. Frühwirth¹, M. Jeitler¹, N. Krammer, I. Krätschmer, D. Liko, T. Madlener, I. Mikulec, N. Rad, J. Schieck¹, R. Schöfbeck, M. Spanring, D. Spitzbart, W. Waltenberger, C.-E. Wulz¹, M. Zarucki

Institute for Nuclear Problems, Minsk, Belarus

V. Drugakov, V. Mossolov, J. Suarez Gonzalez

Universiteit Antwerpen, Antwerpen, Belgium

M.R. Darwish, E.A. De Wolf, D. Di Croce, X. Janssen, J. Lauwers, A. Lelek, M. Pieters, H. Rejeb Sfar, H. Van Haevermaet, P. Van Mechelen, S. Van Putte, N. Van Remortel

Vrije Universiteit Brussel, Brussel, Belgium

F. Blekman, E.S. Bols, S.S. Chhibra, J. D'Hondt, J. De Clercq, D. Lontkovskyi, S. Lowette, I. Marchesini, S. Moortgat, L. Moreels, Q. Python, K. Skovpen, S. Tavernier, W. Van Doninck, P. Van Mulders, I. Van Parijs

Université Libre de Bruxelles, Bruxelles, Belgium

D. Beghin, B. Bilin, H. Brun, B. Clerbaux, G. De Lentdecker, H. Delannoy, B. Dorney, L. Favart, A. Grebenyuk, A.K. Kalsi, J. Luetic, A. Popov, N. Postiau, E. Starling, L. Thomas, C. Vander Velde, P. Vanlaer, D. Vannerom, Q. Wang

Ghent University, Ghent, Belgium

T. Cornelis, D. Dobur, I. Khvastunov², C. Roskas, D. Trocino, M. Tytgat, W. Verbeke, B. Vermassen, M. Vit, N. Zaganidis

Université Catholique de Louvain, Louvain-la-Neuve, Belgium

O. Bondu, G. Bruno, C. Caputo, P. David, C. Delaere, M. Delcourt, A. Giammanco, V. Lemaitre, A. Magitteri, J. Prisciandaro, A. Saggio, M. Vidal Marono, P. Vischia, J. Zobec

Centro Brasileiro de Pesquisas Fisicas, Rio de Janeiro, Brazil

F.L. Alves, G.A. Alves, G. Correia Silva, C. Hensel, A. Moraes, P. Rebello Teles

Universidade do Estado do Rio de Janeiro, Rio de Janeiro, Brazil

E. Belchior Batista Das Chagas, W. Carvalho, J. Chinellato³, E. Coelho, E.M. Da Costa, G.G. Da Silveira⁴, D. De Jesus Damiao, C. De Oliveira Martins, S. Fonseca De Souza, L.M. Huertas Guativa, H. Malbouisson, J. Martins⁵, D. Matos Figueiredo, M. Medina Jaime⁶, M. Melo De Almeida, C. Mora Herrera, L. Mundim, H. Nogima, W.L. Prado Da Silva, L.J. Sanchez Rosas, A. Santoro, A. Sznajder, M. Thiel, E.J. Tonelli Manganote³, F. Torres Da Silva De Araujo, A. Vilela Pereira

Universidade Estadual Paulista ^a, Universidade Federal do ABC ^b, São Paulo, Brazil

S. Ahuja^a, C.A. Bernardes^a, L. Calligaris^a, T.R. Fernandez Perez Tomei^a, E.M. Gregores^b, D.S. Lemos, P.G. Mercadante^b, S.F. Novaes^a, SandraS. Padula^a

Institute for Nuclear Research and Nuclear Energy, Bulgarian Academy of Sciences, Sofia, Bulgaria

A. Aleksandrov, G. Antchev, R. Hadjiiska, P. Iaydjiev, A. Marinov, M. Misheva, M. Rodozov, M. Shopova, G. Sultanov

University of Sofia, Sofia, Bulgaria

M. Bonchev, A. Dimitrov, T. Ivanov, L. Litov, B. Pavlov, P. Petkov

Beihang University, Beijing, China

W. Fang⁷, X. Gao⁷, L. Yuan

Institute of High Energy Physics, Beijing, China

M. Ahmad, G.M. Chen, H.S. Chen, M. Chen, C.H. Jiang, D. Leggat, H. Liao, Z. Liu, S.M. Shaheen⁸, A. Spiezia, J. Tao, E. Yazgan, H. Zhang, S. Zhang⁸, J. Zhao

State Key Laboratory of Nuclear Physics and Technology, Peking University, Beijing, China

A. Agapitos, Y. Ban, G. Chen, A. Levin, J. Li, L. Li, Q. Li, Y. Mao, S.J. Qian, D. Wang

Tsinghua University, Beijing, China

Z. Hu, Y. Wang

Universidad de Los Andes, Bogota, Colombia

C. Avila, A. Cabrera, L.F. Chaparro Sierra, C. Florez, C.F. González Hernández, M.A. Segura Delgado

Universidad de Antioquia, Medellin, Colombia

J. Mejia Guisao, J.D. Ruiz Alvarez, C.A. Salazar González, N. Vanegas Arbelaez

University of Split, Faculty of Electrical Engineering, Mechanical Engineering and Naval Architecture, Split, Croatia

D. Giljanović, N. Godinovic, D. Lelas, I. Puljak, T. Sculac

University of Split, Faculty of Science, Split, Croatia

Z. Antunovic, M. Kovac

Institute Rudjer Boskovic, Zagreb, Croatia

V. Brigljevic, S. Ceci, D. Ferencek, K. Kadija, B. Mesic, M. Roguljic, A. Starodumov⁹, T. Susa

University of Cyprus, Nicosia, Cyprus

M.W. Ather, A. Attikis, E. Erodotou, A. Ioannou, M. Kolosova, S. Konstantinou, G. Mavromanolakis, J. Mousa, C. Nicolaou, F. Ptochos, P.A. Razis, H. Rykaczewski, D. Tsiakkouri

Charles University, Prague, Czech Republic

M. Finger¹⁰, M. Finger Jr.¹⁰, A. Kveton, J. Tomsa

Escuela Politecnica Nacional, Quito, Ecuador

E. Ayala

Universidad San Francisco de Quito, Quito, Ecuador

E. Carrera Jarrin

Academy of Scientific Research and Technology of the Arab Republic of Egypt, Egyptian Network of High Energy Physics, Cairo, Egypt

H. Abdalla¹¹, A. Mohamed¹²

National Institute of Chemical Physics and Biophysics, Tallinn, Estonia

S. Bhowmik, A. Carvalho Antunes De Oliveira, R.K. Dewanjee, K. Ehataht, M. Kadastik, M. Raidal, C. Veelken

Department of Physics, University of Helsinki, Helsinki, Finland

P. Eerola, L. Forthomme, H. Kirschenmann, K. Osterberg, M. Voutilainen

Helsinki Institute of Physics, Helsinki, Finland

F. Garcia, J. Havukainen, J.K. Heikkilä, T. Järvinen, V. Karimäki, R. Kinnunen, T. Lampén, K. Lassila-Perini, S. Laurila, S. Lehti, T. Lindén, P. Luukka, T. Mäenpää, H. Siikonen, E. Tuominen, J. Tuominiemi

Lappeenranta University of Technology, Lappeenranta, Finland

T. Tuuva

IRFU, CEA, Université Paris-Saclay, Gif-sur-Yvette, France

M. Besancon, F. Couderc, M. Dejardin, D. Denegri, B. Fabbro, J.L. Faure, F. Ferri, S. Ganjour, A. Givernaud, P. Gras, G. Hamel de Monchenault, P. Jarry, C. Leloup, E. Locci, J. Malcles, J. Rander, A. Rosowsky, M.Ö. Sahin, A. Savoy-Navarro¹³, M. Titov

Laboratoire Leprince-Ringuet, Ecole polytechnique, CNRS/IN2P3, Université Paris-Saclay, Palaiseau, France

C. Amendola, F. Beaudette, P. Busson, C. Charlot, B. Diab, G. Falmagne, R. Granier de Cassagnac, I. Kucher, A. Lobanov, C. Martin Perez, M. Nguyen, C. Ochando, P. Paganini, J. Rembser, R. Salerno, J.B. Sauvan, Y. Sirois, A. Zabi, A. Zghiche

Université de Strasbourg, CNRS, IPHC UMR 7178, Strasbourg, France

J.-L. Agram¹⁴, J. Andrea, D. Bloch, G. Bourgatte, J.-M. Brom, E.C. Chabert, C. Collard, E. Conte¹⁴, J.-C. Fontaine¹⁴, D. Gelé, U. Goerlach, M. Jansová, A.-C. Le Bihan, N. Tonon, P. Van Hove

Centre de Calcul de l'Institut National de Physique Nucleaire et de Physique des Particules, CNRS/IN2P3, Villeurbanne, France

S. Gadrat

Université de Lyon, Université Claude Bernard Lyon 1, CNRS-IN2P3, Institut de Physique Nucléaire de Lyon, Villeurbanne, France

S. Beauceron, C. Bernet, G. Boudoul, C. Camen, N. Chanon, R. Chierici, D. Contardo, P. Depasse, H. El Mamouni, J. Fay, S. Gascon, M. Gouzevitch, B. Ille, Sa. Jain, F. Lagarde, I.B. Laktineh, H. Lattaud, M. Lethuillier, L. Mirabito, S. Perries, V. Sordini, G. Touquet, M. Vander Donckt, S. Viret

Georgian Technical University, Tbilisi, Georgia

A. Khvedelidze¹⁰

Tbilisi State University, Tbilisi, Georgia

Z. Tsamalaidze¹⁰

RWTH Aachen University, I. Physikalisches Institut, Aachen, Germany

C. Autermann, L. Feld, M.K. Kiesel, K. Klein, M. Lipinski, D. Meuser, A. Pauls, M. Preuten, M.P. Rauch, C. Schomakers, J. Schulz, M. Teroerde, B. Wittmer

RWTH Aachen University, III. Physikalisches Institut A, Aachen, Germany

A. Albert, M. Erdmann, S. Erdweg, T. Esch, B. Fischer, R. Fischer, S. Ghosh, T. Hebbeker, K. Hoepfner, H. Keller, L. Mastrolorenzo, M. Merschmeyer, A. Meyer, P. Millet, G. Mocellin, S. Mondal, S. Mukherjee, D. Noll, A. Novak, T. Pook, A. Pozdnyakov, T. Quast, M. Radziej, Y. Rath, H. Reithler, M. Rieger, J. Roemer, A. Schmidt, S.C. Schuler, A. Sharma, S. Thüer, S. Wiedenbeck

RWTH Aachen University, III. Physikalisches Institut B, Aachen, Germany

G. Flügge, W. Haj Ahmad¹⁵, O. Hlushchenko, T. Kress, T. Müller, A. Nehr Korn, A. Nowack, C. Pistone, O. Pooth, D. Roy, H. Sert, A. Stahl¹⁶

Deutsches Elektronen-Synchrotron, Hamburg, Germany

M. Aldaya Martin, P. Asmuss, I. Babounikau, H. Bakhshiansohi, K. Beernaert, O. Behnke, U. Behrens, A. Bermúdez Martínez, D. Bertsche, A.A. Bin Anuar, K. Borras¹⁷, V. Botta, A. Campbell, A. Cardini, P. Connor, S. Consuegra Rodríguez, C. Contreras-Campana, V. Danilov, A. De Wit, M.M. Defranchis, C. Diez Pardos, D. Domínguez Damiani, G. Eckerlin, D. Eckstein, T. Eichhorn, A. Elwood, E. Eren, E. Gallo¹⁸, A. Geiser, J.M. Grados Luyando, A. Grohsjean, M. Guthoff, M. Haranko, A. Harb, A. Jafari, N.Z. Jomhari, H. Jung, A. Kasem¹⁷, M. Kasemann, H. Kaveh, J. Keaveney, C. Kleinwort, J. Knolle, D. Krücker, W. Lange, T. Lenz, J. Leonard, J. Lidrych, K. Lipka, W. Lohmann¹⁹, R. Mankel, I.-A. Melzer-Pellmann, A.B. Meyer, M. Meyer, M. Missiroli, G. Mittag, J. Mnich, A. Mussgiller, V. Myronenko, D. Pérez Adán, S.K. Pflitsch, D. Pitzl, A. Raspereza, A. Saibel, M. Savitskyi, V. Scheurer, P. Schütze, C. Schwanenberger, R. Shevchenko, A. Singh, H. Tholen, O. Turkot, A. Vagnerini, M. Van De Klundert, G.P. Van Onsem, R. Walsh, Y. Wen, K. Wichmann, C. Wissing, O. Zenaiev, R. Zlebcik

University of Hamburg, Hamburg, Germany

R. Aggleton, S. Bein, L. Benato, A. Benecke, V. Blobel, T. Dreyer, A. Ebrahimi, A. Fröhlich, C. Garbers, E. Garutti, D. Gonzalez, P. Gunnellini, J. Haller, A. Hinzmann, A. Karavdina, G. Kasieczka, R. Klanner, R. Kogler, N. Kovalchuk, S. Kurz, V. Kutzner, J. Lange, T. Lange, A. Malara, D. Marconi, J. Multhaupt, M. Niedziela, C.E.N. Niemeyer, D. Nowatschin, A. Perieanu, A. Reimers, O. Rieger, C. Scharf, P. Schleper, S. Schumann, J. Schwandt, J. Sonneveld, H. Stadie, G. Steinbrück, F.M. Stober, M. Stöver, B. Vormwald, I. Zoi

Karlsruher Institut fuer Technologie, Karlsruhe, Germany

M. Akbiyik, C. Barth, M. Baselga, S. Baur, T. Berger, E. Butz, R. Caspart, T. Chwalek, W. De Boer, A. Dierlamm, K. El Morabit, N. Faltermann, M. Giffels, P. Goldenzweig, A. Gottmann, M.A. Harrendorf, F. Hartmann¹⁶, U. Husemann, S. Kudella, S. Mitra, M.U. Mozer, Th. Müller, M. Musich, A. Nürnberg, G. Quast, K. Rabbertz, M. Schröder, I. Shvetsov, H.J. Simonis, R. Ulrich, M. Weber, C. Wöhrmann, R. Wolf

Institute of Nuclear and Particle Physics (INPP), NCSR Demokritos, Aghia Paraskevi, Greece

G. Anagnostou, P. Asenov, G. Daskalakis, T. Geralis, A. Kyriakis, D. Loukas, G. Paspalaki

National and Kapodistrian University of Athens, Athens, Greece

M. Diamantopoulou, G. Karathanasis, P. Kontaxakis, A. Panagiotou, I. Papavergou, N. Saoulidou, A. Stakia, K. Theofilatos, K. Vellidis

National Technical University of Athens, Athens, Greece

G. Bakas, K. Kousouris, I. Papakrivopoulos, G. Tsipolitis

University of Ioánnina, Ioánnina, Greece

I. Evangelou, C. Foudas, P. Giannelis, P. Katsoulis, P. Kokkas, S. Mallios, K. Manitará, N. Manthos, I. Papadopoulos, J. Strogas, F.A. Triantis, D. Tsitsonis

MTA-ELTE Lendület CMS Particle and Nuclear Physics Group, Eötvös Loránd University, Budapest, Hungary

M. Bartók²⁰, M. Csanad, P. Major, K. Mandal, A. Mehta, M.I. Nagy, G. Pasztor, O. Surányi, G.I. Veres

Wigner Research Centre for Physics, Budapest, Hungary

G. Bencze, C. Hajdu, D. Horvath²¹, F. Sikler, T. Vámi, V. Veszpremi, G. Vesztergombi[†]

Institute of Nuclear Research ATOMKI, Debrecen, Hungary

N. Beni, S. Czellar, J. Karancsi²⁰, A. Makovec, J. Molnar, Z. Szillasi

Institute of Physics, University of Debrecen, Debrecen, Hungary

P. Raics, D. Teyssier, Z.L. Trocsanyi, B. Ujvari

Eszterhazy Karoly University, Karoly Robert Campus, Gyongyos, Hungary

T. Csorgo, W.J. Metzger, F. Nemes, T. Novak

Indian Institute of Science (IISc), Bangalore, India

S. Choudhury, J.R. Komaragiri, P.C. Tiwari

National Institute of Science Education and Research, HBNI, Bhubaneswar, India

S. Bahinipati²³, C. Kar, G. Kole, P. Mal, V.K. Muraleedharan Nair Bindhu, A. Nayak²⁴, D.K. Sahoo²³, S.K. Swain

Panjab University, Chandigarh, India

S. Bansal, S.B. Beri, V. Bhatnagar, S. Chauhan, R. Chawla, N. Dhingra, R. Gupta, A. Kaur, M. Kaur, S. Kaur, P. Kumari, M. Lohan, M. Meena, K. Sandeep, S. Sharma, J.B. Singh, A.K. Viridi, G. Walia

University of Delhi, Delhi, India

A. Bhardwaj, B.C. Choudhary, R.B. Garg, M. Gola, S. Keshri, Ashok Kumar, S. Malhotra, M. Naimuddin, P. Priyanka, K. Ranjan, Aashaq Shah, R. Sharma

Saha Institute of Nuclear Physics, HBNI, Kolkata, India

R. Bhardwaj²⁵, M. Bharti²⁵, R. Bhattacharya, S. Bhattacharya, U. Bhawandeep²⁵, D. Bhowmik, S. Dey, S. Dutta, S. Ghosh, M. Maity²⁶, K. Mondal, S. Nandan, A. Purohit, P.K. Rout, G. Saha, S. Sarkar, T. Sarkar²⁶, M. Sharan, B. Singh²⁵, S. Thakur²⁵

Indian Institute of Technology Madras, Madras, India

P.K. Behera, P. Kalbhor, A. Muhammad, P.R. Pujahari, A. Sharma, A.K. Sikdar

Bhabha Atomic Research Centre, Mumbai, India

R. Chudasama, D. Dutta, V. Jha, V. Kumar, D.K. Mishra, P.K. Netrakanti, L.M. Pant, P. Shukla

Tata Institute of Fundamental Research-A, Mumbai, India

T. Aziz, M.A. Bhat, S. Dugad, G.B. Mohanty, N. Sur, RavindraKumar Verma

Tata Institute of Fundamental Research-B, Mumbai, India

S. Banerjee, S. Bhattacharya, S. Chatterjee, P. Das, M. Guchait, S. Karmakar, S. Kumar, G. Majumder, K. Mazumdar, N. Sahoo, S. Sawant

Indian Institute of Science Education and Research (IISER), Pune, India

S. Chauhan, S. Dube, V. Hegde, A. Kapoor, K. Kothekar, S. Pandey, A. Rane, A. Rastogi, S. Sharma

Institute for Research in Fundamental Sciences (IPM), Tehran, Iran

S. Chenarani²⁷, E. Eskandari Tadavani, S.M. Etesami²⁷, M. Khakzad, M. Mohammadi Najafabadi, M. Naseri, F. Rezaei Hosseinabadi

University College Dublin, Dublin, Ireland

M. Felcini, M. Grunewald

INFN Sezione di Bari ^a, Università di Bari ^b, Politecnico di Bari ^c, Bari, Italy

M. Abbrescia^{a,b}, C. Calabria^{a,b}, A. Colaleo^a, D. Creanza^{a,c}, L. Cristella^{a,b}, N. De Filippis^{a,c}, M. De Palma^{a,b}, A. Di Florio^{a,b}, L. Fiore^a, A. Gelmi^{a,b}, G. Iaselli^{a,c}, M. Ince^{a,b}, S. Lezki^{a,b},

G. Maggi^{a,c}, M. Maggi^a, G. Miniello^{a,b}, S. My^{a,b}, S. Nuzzo^{a,b}, A. Pompili^{a,b}, G. Pugliese^{a,c}, R. Radogna^a, A. Ranieri^a, G. Selvaggi^{a,b}, L. Silvestris^a, R. Venditti^a, P. Verwilligen^a

INFN Sezione di Bologna ^a, Università di Bologna ^b, Bologna, Italy

G. Abbiendi^a, C. Battilana^{a,b}, D. Bonacorsi^{a,b}, L. Borgonovi^{a,b}, S. Braibant-Giacomelli^{a,b}, R. Campanini^{a,b}, P. Capiluppi^{a,b}, A. Castro^{a,b}, F.R. Cavallo^a, C. Ciocca^a, G. Codispoti^{a,b}, M. Cuffiani^{a,b}, G.M. Dallavalle^a, F. Fabbri^a, A. Fanfani^{a,b}, E. Fontanesi, P. Giacomelli^a, C. Grandi^a, L. Guiducci^{a,b}, F. Iemmi^{a,b}, S. Lo Meo^{a,28}, S. Marcellini^a, G. Masetti^a, F.L. Navarria^{a,b}, A. Perrotta^a, F. Primavera^{a,b}, A.M. Rossi^{a,b}, T. Rovelli^{a,b}, G.P. Siroli^{a,b}, N. Tosi^a

INFN Sezione di Catania ^a, Università di Catania ^b, Catania, Italy

S. Albergo^{a,b,29}, S. Costa^{a,b}, A. Di Mattia^a, R. Potenza^{a,b}, A. Tricomi^{a,b,29}, C. Tuve^{a,b}

INFN Sezione di Firenze ^a, Università di Firenze ^b, Firenze, Italy

G. Barbagli^a, R. Ceccarelli, K. Chatterjee^{a,b}, V. Ciulli^{a,b}, C. Civinini^a, R. D'Alessandro^{a,b}, E. Focardi^{a,b}, G. Latino, P. Lenzi^{a,b}, M. Meschini^a, S. Paoletti^a, G. Sguazzoni^a, D. Strom^a, L. Viliani^a

INFN Laboratori Nazionali di Frascati, Frascati, Italy

L. Benussi, S. Bianco, D. Piccolo

INFN Sezione di Genova ^a, Università di Genova ^b, Genova, Italy

M. Bozzo^{a,b}, F. Ferro^a, R. Mulargia^{a,b}, E. Robutti^a, S. Tosi^{a,b}

INFN Sezione di Milano-Bicocca ^a, Università di Milano-Bicocca ^b, Milano, Italy

A. Benaglia^a, A. Beschi^{a,b}, F. Brivio^{a,b}, V. Ciriolo^{a,b,16}, S. Di Guida^{a,b,16}, M.E. Dinardo^{a,b}, P. Dini^a, S. Fiorendi^{a,b}, S. Gennai^a, A. Ghezzi^{a,b}, P. Govoni^{a,b}, L. Guzzi^{a,b}, M. Malberti^a, S. Malvezzi^a, D. Menasce^a, F. Monti^{a,b}, L. Moroni^a, G. Ortona^{a,b}, M. Paganoni^{a,b}, D. Pedrini^a, S. Ragazzi^{a,b}, T. Tabarelli de Fatis^{a,b}, D. Zuolo^{a,b}

INFN Sezione di Napoli ^a, Università di Napoli 'Federico II' ^b, Napoli, Italy, Università della Basilicata ^c, Potenza, Italy, Università G. Marconi ^d, Roma, Italy

S. Buontempo^a, N. Cavallo^{a,c}, A. De Iorio^{a,b}, A. Di Crescenzo^{a,b}, F. Fabozzi^{a,c}, F. Fienga^a, G. Galati^a, A.O.M. Iorio^{a,b}, L. Lista^{a,b}, S. Meola^{a,d,16}, P. Paolucci^{a,16}, B. Rossi^a, C. Sciacca^{a,b}, E. Voevodina^{a,b}

INFN Sezione di Padova ^a, Università di Padova ^b, Padova, Italy, Università di Trento ^c, Trento, Italy

P. Azzi^a, N. Bacchetta^a, D. Bisello^{a,b}, A. Boletti^{a,b}, A. Bragagnolo, R. Carlin^{a,b}, P. Checchia^a, P. De Castro Manzano^a, T. Dorigo^a, U. Dosselli^a, F. Gasparini^{a,b}, U. Gasparini^{a,b}, A. Gozzelino^a, S.Y. Hoh, P. Lujan, M. Margoni^{a,b}, A.T. Meneguzzo^{a,b}, J. Pazzini^{a,b}, M. Presilla^b, P. Ronchese^{a,b}, R. Rossin^{a,b}, F. Simonetto^{a,b}, A. Tiko, M. Tosi^{a,b}, M. Zanetti^{a,b}, P. Zotto^{a,b}, G. Zumerle^{a,b}

INFN Sezione di Pavia ^a, Università di Pavia ^b, Pavia, Italy

A. Braghieri^a, P. Montagna^{a,b}, S.P. Ratti^{a,b}, V. Re^a, M. Ressegotti^{a,b}, C. Riccardi^{a,b}, P. Salvini^a, I. Vai^{a,b}, P. Vitulo^{a,b}

INFN Sezione di Perugia ^a, Università di Perugia ^b, Perugia, Italy

M. Biasini^{a,b}, G.M. Bilei^a, C. Cecchi^{a,b}, D. Ciangottini^{a,b}, L. Fanò^{a,b}, P. Lariccia^{a,b}, R. Leonardi^{a,b}, E. Manoni^a, G. Mantovani^{a,b}, V. Mariani^{a,b}, M. Menichelli^a, A. Rossi^{a,b}, A. Santocchia^{a,b}, D. Spiga^a

INFN Sezione di Pisa ^a, Università di Pisa ^b, Scuola Normale Superiore di Pisa ^c, Pisa, Italy

K. Androsov^a, P. Azzurri^a, G. Bagliesi^a, V. Bertacchi^{a,c}, L. Bianchini^a, T. Boccali^a, R. Castaldi^a, M.A. Ciocci^{a,b}, R. Dell'Orso^a, G. Fedi^a, L. Giannini^{a,c}, A. Giassi^a, M.T. Grippo^a,

F. Ligabue^{a,c}, E. Manca^{a,c}, G. Mandorli^{a,c}, A. Messineo^{a,b}, F. Palla^a, A. Rizzi^{a,b}, G. Rolandi³⁰, S. Roy Chowdhury, A. Scribano^a, P. Spagnolo^a, R. Tenchini^a, G. Tonelli^{a,b}, N. Turini, A. Venturi^a, P.G. Verdini^a

INFN Sezione di Roma ^a, Sapienza Università di Roma ^b, Rome, Italy

F. Cavallari^a, M. Cipriani^{a,b}, D. Del Re^{a,b}, E. Di Marco^{a,b}, M. Diemoz^a, E. Longo^{a,b}, B. Marzocchi^{a,b}, P. Meridiani^a, G. Organtini^{a,b}, F. Pandolfi^a, R. Paramatti^{a,b}, C. Quaranta^{a,b}, S. Rahatlou^{a,b}, C. Rovelli^a, F. Santanastasio^{a,b}, L. Soffi^{a,b}

INFN Sezione di Torino ^a, Università di Torino ^b, Torino, Italy, Università del Piemonte Orientale ^c, Novara, Italy

N. Amapane^{a,b}, R. Arcidiacono^{a,c}, S. Argiro^{a,b}, M. Arneodo^{a,c}, N. Bartosik^a, R. Bellan^{a,b}, C. Biino^a, A. Cappati^{a,b}, N. Cartiglia^a, S. Cometti^a, M. Costa^{a,b}, R. Covarelli^{a,b}, N. Demaria^a, B. Kiani^{a,b}, C. Mariotti^a, S. Maselli^a, E. Migliore^{a,b}, V. Monaco^{a,b}, E. Monteil^{a,b}, M. Monteno^a, M.M. Obertino^{a,b}, L. Pacher^{a,b}, N. Pastrone^a, M. Pelliccioni^a, G.L. Pinna Angioni^{a,b}, A. Romero^{a,b}, M. Ruspà^{a,c}, R. Sacchi^{a,b}, R. Salvatico^{a,b}, V. Sola^a, A. Solano^{a,b}, D. Soldi^{a,b}, A. Staiano^a

INFN Sezione di Trieste ^a, Università di Trieste ^b, Trieste, Italy

S. Belforte^a, V. Candelise^{a,b}, M. Casarsa^a, F. Cossutti^a, A. Da Rold^{a,b}, G. Della Ricca^{a,b}, F. Vazzoler^{a,b}, A. Zanetti^a

Kyungpook National University, Daegu, Korea

B. Kim, D.H. Kim, G.N. Kim, M.S. Kim, J. Lee, S.W. Lee, C.S. Moon, Y.D. Oh, S.I. Pak, S. Sekmen, D.C. Son, Y.C. Yang

Chonnam National University, Institute for Universe and Elementary Particles, Kwangju, Korea

H. Kim, D.H. Moon, G. Oh

Hanyang University, Seoul, Korea

B. Francois, T.J. Kim, J. Park

Korea University, Seoul, Korea

S. Cho, S. Choi, Y. Go, D. Gyun, S. Ha, B. Hong, K. Lee, K.S. Lee, J. Lim, J. Park, S.K. Park, Y. Roh

Kyung Hee University, Department of Physics

J. Goh

Sejong University, Seoul, Korea

H.S. Kim

Seoul National University, Seoul, Korea

J. Almond, J.H. Bhyun, J. Choi, S. Jeon, J. Kim, J.S. Kim, H. Lee, K. Lee, S. Lee, K. Nam, M. Oh, S.B. Oh, B.C. Radburn-Smith, U.K. Yang, H.D. Yoo, I. Yoon, G.B. Yu

University of Seoul, Seoul, Korea

D. Jeon, H. Kim, J.H. Kim, J.S.H. Lee, I.C. Park, I. Watson

Sungkyunkwan University, Suwon, Korea

Y. Choi, C. Hwang, Y. Jeong, J. Lee, Y. Lee, I. Yu

Riga Technical University, Riga, Latvia

V. Veckalns³¹

Vilnius University, Vilnius, Lithuania

V. Dudenas, A. Juodagalvis, G. Tamulaitis, J. Vaitkus

National Centre for Particle Physics, Universiti Malaya, Kuala Lumpur, Malaysia

Z.A. Ibrahim, F. Mohamad Idris³², W.A.T. Wan Abdullah, M.N. Yusli, Z. Zolkapli

Universidad de Sonora (UNISON), Hermosillo, Mexico

J.F. Benitez, A. Castaneda Hernandez, J.A. Murillo Quijada, L. Valencia Palomo

Centro de Investigacion y de Estudios Avanzados del IPN, Mexico City, Mexico

H. Castilla-Valdez, E. De La Cruz-Burelo, I. Heredia-De La Cruz³³, R. Lopez-Fernandez, A. Sanchez-Hernandez

Universidad Iberoamericana, Mexico City, Mexico

S. Carrillo Moreno, C. Oropeza Barrera, M. Ramirez-Garcia, F. Vazquez Valencia

Benemerita Universidad Autonoma de Puebla, Puebla, Mexico

J. Eysermans, I. Pedraza, H.A. Salazar Ibarquen, C. Uribe Estrada

Universidad Autónoma de San Luis Potosí, San Luis Potosí, Mexico

A. Morelos Pineda

University of Montenegro, Podgorica, Montenegro

N. Raicevic

University of Auckland, Auckland, New Zealand

D. Krofcheck

University of Canterbury, Christchurch, New Zealand

S. Bheesette, P.H. Butler

National Centre for Physics, Quaid-I-Azam University, Islamabad, Pakistan

A. Ahmad, M. Ahmad, Q. Hassan, H.R. Hoorani, W.A. Khan, M.A. Shah, M. Shoaib, M. Waqas

AGH University of Science and Technology Faculty of Computer Science, Electronics and Telecommunications, Krakow, Poland

V. Avati, L. Grzanka, M. Malawski

National Centre for Nuclear Research, Swierk, Poland

H. Bialkowska, M. Bluj, B. Boimska, M. Górski, M. Kazana, M. Szleper, P. Zalewski

Institute of Experimental Physics, Faculty of Physics, University of Warsaw, Warsaw, Poland

K. Bunkowski, A. Byzuk³⁴, K. Doroba, A. Kalinowski, M. Konecki, J. Krolikowski, M. Misiura, M. Olszewski, A. Pyskir, M. Walczak

Laboratório de Instrumentação e Física Experimental de Partículas, Lisboa, Portugal

M. Araujo, P. Bargassa, D. Bastos, A. Di Francesco, P. Faccioli, B. Galinhas, M. Gallinaro, J. Hollar, N. Leonardo, J. Seixas, K. Shchelina, G. Strong, O. Toldaiev, J. Varela

Joint Institute for Nuclear Research, Dubna, Russia

P. Bunin, M. Gavrilenko, A. Golunov, I. Golutvin, N. Gorbounov, I. Gorbunov, A. Kamenev, V. Karjavine, V. Korenkov, A. Lanev, A. Malakhov, V. Matveev^{35,36}, P. Moisezenz, V. Palichik, V. Perelygin, M. Savina, S. Shmatov, S. Shulha, V. Trofimov, A. Zarubin

Petersburg Nuclear Physics Institute, Gatchina (St. Petersburg), Russia

L. Chtchipounov, V. Golovtsov, Y. Ivanov, V. Kim³⁷, E. Kuznetsova³⁸, P. Levchenko, V. Murzin, V. Oreshkin, I. Smirnov, D. Sosnov, V. Sulimov, L. Uvarov, A. Vorobyev

Institute for Nuclear Research, Moscow, Russia

Yu. Andreev, A. Dermenev, S. Gninenko, N. Golubev, A. Karneyeu, M. Kirsanov, N. Krasnikov, A. Pashenkov, D. Tlisov, A. Toropin

Institute for Theoretical and Experimental Physics named by A.I. Alikhanov of NRC 'Kurchatov Institute', Moscow, Russia

V. Epshteyn, V. Gavrilov, N. Lychkovskaya, A. Nikitenko³⁹, V. Popov, I. Pozdnyakov, G. Safronov, A. Spiridonov, A. Stepenov, M. Toms, E. Vlasov, A. Zhokin

Moscow Institute of Physics and Technology, Moscow, Russia

T. Aushev

National Research Nuclear University 'Moscow Engineering Physics Institute' (MEPhI), Moscow, Russia

M. Chadeeva⁴⁰, P. Parygin, D. Philippov, E. Popova, V. Rusinov

P.N. Lebedev Physical Institute, Moscow, Russia

V. Andreev, M. Azarkin, I. Dremin, M. Kirakosyan, A. Terkulov

Skobeltsyn Institute of Nuclear Physics, Lomonosov Moscow State University, Moscow, Russia

A. Belyaev, E. Boos, V. Bunichev, M. Dubinin⁴¹, L. Dudko, A. Gribushin, V. Klyukhin, O. Kodolova, I. Lokhtin, S. Obraztsov, M. Perfilov, S. Petrushanko, V. Savrin

Novosibirsk State University (NSU), Novosibirsk, Russia

A. Barnyakov⁴², V. Blinov⁴², T. Dimova⁴², L. Kardapol'tsev⁴², Y. Skovpen⁴²

Institute for High Energy Physics of National Research Centre 'Kurchatov Institute', Protvino, Russia

I. Azhgirey, I. Bayshev, S. Bitioukov, V. Kachanov, D. Konstantinov, P. Mandrik, V. Petrov, R. Ryutin, S. Slabospitskii, A. Sobol, S. Troshin, N. Tyurin, A. Uzunian, A. Volkov

National Research Tomsk Polytechnic University, Tomsk, Russia

A. Babaev, A. Iuzhakov, V. Okhotnikov

Tomsk State University, Tomsk, Russia

V. Borchsh, V. Ivanchenko, E. Tcherniaev

University of Belgrade: Faculty of Physics and VINCA Institute of Nuclear Sciences

P. Adzic⁴³, P. Cirkovic, D. Devetak, M. Dordevic, P. Milenovic, J. Milosevic, M. Stojanovic

Centro de Investigaciones Energéticas Medioambientales y Tecnológicas (CIEMAT), Madrid, Spain

M. Aguilar-Benitez, J. Alcaraz Maestre, A. Alvarez Fernández, I. Bachiller, M. Barrio Luna, J.A. Brochero Cifuentes, C.A. Carrillo Montoya, M. Cepeda, M. Cerrada, N. Colino, B. De La Cruz, A. Delgado Peris, C. Fernandez Bedoya, J.P. Fernández Ramos, J. Flix, M.C. Fouz, O. Gonzalez Lopez, S. Goy Lopez, J.M. Hernandez, M.I. Josa, D. Moran, . Navarro Tobar, A. Pérez-Calero Yzquierdo, J. Puerta Pelayo, I. Redondo, L. Romero, S. Sánchez Navas, M.S. Soares, A. Triossi, C. Willmott

Universidad Autónoma de Madrid, Madrid, Spain

C. Albajar, J.F. de Trocóniz

Universidad de Oviedo, Instituto Universitario de Ciencias y Tecnologías Espaciales de Asturias (ICTEA), Oviedo, Spain

B. Alvarez Gonzalez, J. Cuevas, C. Erice, J. Fernandez Menendez, S. Folgueras,

I. Gonzalez Caballero, J.R. González Fernández, E. Palencia Cortezon, V. Rodríguez Bouza, S. Sanchez Cruz

Instituto de Física de Cantabria (IFCA), CSIC-Universidad de Cantabria, Santander, Spain

I.J. Cabrillo,
A. Calderon, B. Chazin Quero, J. Duarte Campderros, M. Fernandez, P.J. Fernández Manteca, A. García Alonso, G. Gomez, C. Martinez Rivero, P. Martinez Ruiz del Arbol, F. Matorras, J. Piedra Gomez, C. Prieels, T. Rodrigo, A. Ruiz-Jimeno, L. Russo⁴⁴, L. Scodellaro, N. Trevisani, I. Vila, J.M. Vizan Garcia

University of Colombo, Colombo, Sri Lanka

K. Malagalage

University of Ruhuna, Department of Physics, Matara, Sri Lanka

W.G.D. Dharmaratna, N. Wickramage

CERN, European Organization for Nuclear Research, Geneva, Switzerland

D. Abbaneo, B. Akgun, E. Auffray, G. Auzinger, J. Baechler, P. Baillon, A.H. Ball, D. Barney, J. Bendavid, M. Bianco, A. Bocci, E. Bossini, C. Botta, E. Brondolin, T. Camporesi, A. Caratelli, G. Cerminara, E. Chapon, G. Cucciati, D. d'Enterria, A. Dabrowski, N. Daci, V. Daponte, A. David, O. Davignon, A. De Roeck, N. Deelen, M. Deile, M. Dobson, M. Dünser, N. Dupont, A. Elliott-Peisert, F. Fallavollita⁴⁵, D. Fasanella, G. Franzoni, J. Fulcher, W. Funk, S. Giani, D. Gigi, A. Gilbert, K. Gill, F. Glege, M. Gruchala, M. Guilbaud, D. Gulhan, J. Hegeman, C. Heidegger, Y. Iiyama, V. Innocente, P. Janot, O. Karacheban¹⁹, J. Kaspar, J. Kieseler, M. Krammer¹, C. Lange, P. Lecoq, C. Lourenço, L. Malgeri, M. Mannelli, A. Massironi, F. Meijers, J.A. Merlin, S. Mersi, E. Meschi, F. Moortgat, M. Mulders, J. Ngadiuba, S. Nourbakhsh, S. Orfanelli, L. Orsini, F. Pantaleo¹⁶, L. Pape, E. Perez, M. Peruzzi, A. Petrilli, G. Petrucciani, A. Pfeiffer, M. Pierini, F.M. Pitters, D. Rabady, A. Racz, M. Rovere, H. Sakulin, C. Schäfer, C. Schwick, M. Selvaggi, A. Sharma, P. Silva, W. Snoeys, P. Sphicas⁴⁶, J. Steggemann, V.R. Tavolaro, D. Treille, A. Tsirou, A. Vartak, M. Verzetti, W.D. Zeuner

Paul Scherrer Institut, Villigen, Switzerland

L. Caminada⁴⁷, K. Deiters, W. Erdmann, R. Horisberger, Q. Ingram, H.C. Kaestli, D. Kotlinski, U. Langenegger, T. Rohe, S.A. Wiederkehr

ETH Zurich - Institute for Particle Physics and Astrophysics (IPA), Zurich, Switzerland

M. Backhaus, P. Berger, N. Chernyavskaya, G. Dissertori, M. Dittmar, M. Donegà, C. Dorfer, T.A. Gómez Espinosa, C. Grab, D. Hits, T. Klijnsma, W. Lustermaan, R.A. Manzoni, M. Marionneau, M.T. Meinhard, F. Micheli, P. Musella, F. Nessi-Tedaldi, F. Pauss, G. Perrin, L. Perrozzi, S. Pigazzini, M. Reichmann, C. Reissel, T. Reitenspiess, D. Ruini, D.A. Sanz Becerra, M. Schönenberger, L. Shchutska, M.L. Vesterbacka Olsson, R. Wallny, D.H. Zhu

Universität Zürich, Zurich, Switzerland

T.K. Aarrestad, C. Amsler⁴⁸, D. Brzhechko, M.F. Canelli, A. De Cosa, R. Del Burgo, S. Donato, B. Kilminster, S. Leontsinis, V.M. Mikuni, I. Neutelings, G. Rauco, P. Robmann, D. Salerno, K. Schweiger, C. Seitz, Y. Takahashi, S. Wertz, A. Zucchetta

National Central University, Chung-Li, Taiwan

T.H. Doan, C.M. Kuo, W. Lin, A. Roy, S.S. Yu

National Taiwan University (NTU), Taipei, Taiwan

P. Chang, Y. Chao, K.F. Chen, P.H. Chen, W.-S. Hou, Y.y. Li, R.-S. Lu, E. Paganis, A. Psallidas, A. Steen

Chulalongkorn University, Faculty of Science, Department of Physics, Bangkok, Thailand

B. Asavapibhop, C. Asawatangtrakuldee, N. Srimanobhas, N. Suwonjandee

ukurova University, Physics Department, Science and Art Faculty, Adana, Turkey

A. Bat, F. Boran, S. Cerci⁴⁹, S. Damarseckin⁵⁰, Z.S. Demiroglu, F. Dolek, C. Dozen, I. Dumanoglu, G. Gokbulut, EmineGurpinar Guler⁵¹, Y. Guler, I. Hos⁵², C. Isik, E.E. Kangal⁵³, O. Kara, A. Kayis Topaksu, U. Kiminsu, M. Oglakci, G. Onengut, K. Ozdemir⁵⁴, S. Ozturk⁵⁵, A.E. Simsek, D. Sunar Cerci⁴⁹, U.G. Tok, S. Turkcapar, I.S. Zorbakir, C. Zorbilmez

Middle East Technical University, Physics Department, Ankara, Turkey

B. Isildak⁵⁶, G. Karapinar⁵⁷, M. Yalvac

Bogazici University, Istanbul, Turkey

I.O. Atakisi, E. Gülmez, M. Kaya⁵⁸, O. Kaya⁵⁹, B. Kaynak, Ö. Özçelik, S. Tekten, E.A. Yetkin⁶⁰

Istanbul Technical University, Istanbul, Turkey

A. Cakir, K. Cankocak, Y. Komurcu, S. Sen⁶¹

Istanbul University, Istanbul, Turkey

S. Ozkorucuklu

Institute for Scintillation Materials of National Academy of Science of Ukraine, Kharkov, Ukraine

B. Grynyov

National Scientific Center, Kharkov Institute of Physics and Technology, Kharkov, Ukraine

L. Levchuk

University of Bristol, Bristol, United Kingdom

F. Ball, E. Bhal, S. Bologna, J.J. Brooke, D. Burns, E. Clement, D. Cussans, H. Flacher, J. Goldstein, G.P. Heath, H.F. Heath, L. Kreczko, S. Paramesvaran, B. Penning, T. Sakuma, S. Seif El Nasr-Storey, D. Smith, V.J. Smith, J. Taylor, A. Titterton

Rutherford Appleton Laboratory, Didcot, United Kingdom

K.W. Bell, A. Belyaev⁶², C. Brew, R.M. Brown, D. Cieri, D.J.A. Cockerill, J.A. Coughlan, K. Harder, S. Harper, J. Linacre, K. Manolopoulos, D.M. Newbold, E. Olaiya, D. Petyt, T. Reis, T. Schuh, C.H. Shepherd-Themistocleous, A. Thea, I.R. Tomalin, T. Williams, W.J. Womersley

Imperial College, London, United Kingdom

R. Bainbridge, P. Bloch, J. Borg, S. Breeze, O. Buchmuller, A. Bundock, GurpreetSingh CHAHAL⁶³, D. Colling, P. Dauncey, G. Davies, M. Della Negra, R. Di Maria, P. Everaerts, G. Hall, G. Iles, T. James, M. Komm, C. Laner, L. Lyons, A.-M. Magnan, S. Malik, A. Martelli, V. Milosevic, J. Nash⁶⁴, V. Palladino, M. Pesaresi, D.M. Raymond, A. Richards, A. Rose, E. Scott, C. Seez, A. Shtipliyski, M. Stoye, T. Strebler, S. Summers, A. Tapper, K. Uchida, T. Virdee¹⁶, N. Wardle, D. Winterbottom, J. Wright, A.G. Zecchinelli, S.C. Zenz

Brunel University, Uxbridge, United Kingdom

J.E. Cole, P.R. Hobson, A. Khan, P. Kyberd, C.K. Mackay, A. Morton, I.D. Reid, L. Teodorescu, S. Zahid

Baylor University, Waco, USA

K. Call, J. Dittmann, K. Hatakeyama, C. Madrid, B. McMaster, N. Pastika, C. Smith

Catholic University of America, Washington, DC, USA

R. Bartek, A. Dominguez, R. Uniyal

The University of Alabama, Tuscaloosa, USA

A. Buccilli, S.I. Cooper, C. Henderson, P. Rumerio, C. West

Boston University, Boston, USA

D. Arcaro, T. Bose, Z. Demiragli, D. Gastler, S. Girgis, D. Pinna, C. Richardson, J. Rohlf, D. Sperka, I. Suarez, L. Sulak, D. Zou

Brown University, Providence, USA

G. Benelli, B. Burkle, X. Coubez, D. Cutts, Y.t. Duh, M. Hadley, J. Hakala, U. Heintz, J.M. Hogan⁶⁵, K.H.M. Kwok, E. Laird, G. Landsberg, J. Lee, Z. Mao, M. Narain, S. Sagir⁶⁶, R. Syarif, E. Usai, D. Yu

University of California, Davis, Davis, USA

R. Band, C. Brainerd, R. Breedon, M. Calderon De La Barca Sanchez, M. Chertok, J. Conway, R. Conway, P.T. Cox, R. Erbacher, C. Flores, G. Funk, F. Jensen, W. Ko, O. Kukral, R. Lander, M. Mulhearn, D. Pellett, J. Pilot, M. Shi, D. Stolp, D. Taylor, K. Tos, M. Tripathi, Z. Wang, F. Zhang

University of California, Los Angeles, USA

M. Bachtis, C. Bravo, R. Cousins, A. Dasgupta, A. Florent, J. Hauser, M. Ignatenko, N. Mccoll, W.A. Nash, S. Regnard, D. Saltzberg, C. Schnaible, B. Stone, V. Valuev

University of California, Riverside, Riverside, USA

K. Burt, R. Clare, J.W. Gary, S.M.A. Ghiasi Shirazi, G. Hanson, G. Karapostoli, E. Kennedy, O.R. Long, M. Olmedo Negrete, M.I. Paneva, W. Si, L. Wang, H. Wei, S. Wimpenny, B.R. Yates, Y. Zhang

University of California, San Diego, La Jolla, USA

J.G. Branson, P. Chang, S. Cittolin, M. Derdzinski, R. Gerosa, D. Gilbert, B. Hashemi, D. Klein, V. Krutelyov, J. Letts, M. Masciovecchio, S. May, S. Padhi, M. Pieri, V. Sharma, M. Tadel, F. Würthwein, A. Yagil, G. Zevi Della Porta

University of California, Santa Barbara - Department of Physics, Santa Barbara, USA

N. Amin, R. Bhandari, C. Campagnari, M. Citron, V. Dutta, M. Franco Sevilla, L. Gouskos, J. Incandela, B. Marsh, H. Mei, A. Ovcharova, H. Qu, J. Richman, U. Sarica, D. Stuart, S. Wang, J. Yoo

California Institute of Technology, Pasadena, USA

D. Anderson, A. Bornheim, O. Cerri, I. Dutta, J.M. Lawhorn, N. Lu, J. Mao, H.B. Newman, T.Q. Nguyen, J. Pata, M. Spiropulu, J.R. Vlimant, S. Xie, Z. Zhang, R.Y. Zhu

Carnegie Mellon University, Pittsburgh, USA

M.B. Andrews, T. Ferguson, T. Mudholkar, M. Paulini, M. Sun, I. Vorobiev, M. Weinberg

University of Colorado Boulder, Boulder, USA

J.P. Cumalat, W.T. Ford, A. Johnson, E. MacDonald, T. Mulholland, R. Patel, A. Perloff, K. Stenson, K.A. Ulmer, S.R. Wagner

Cornell University, Ithaca, USA

J. Alexander, J. Chaves, Y. Cheng, J. Chu, A. Datta, A. Frankenthal, K. Mcdermott, N. Mirman, J.R. Patterson, D. Quach, A. Rinkevicius⁶⁷, A. Ryd, S.M. Tan, Z. Tao, J. Thom, P. Wittich, M. Zientek

Fermi National Accelerator Laboratory, Batavia, USA

S. Abdullin, M. Albrow, M. Alyari, G. Apollinari, A. Apresyan, A. Apyan, S. Banerjee,

L.A.T. Bauerdick, A. Beretvas, J. Berryhill, P.C. Bhat, K. Burkett, J.N. Butler, A. Canepa, G.B. Cerati, H.W.K. Cheung, F. Chlebana, M. Cremonesi, J. Duarte, V.D. Elvira, J. Freeman, Z. Gece, E. Gottschalk, L. Gray, D. Green, S. Grünendahl, O. Gutsche, AllisonReinsvold Hall, J. Hanlon, R.M. Harris, S. Hasegawa, R. Heller, J. Hirschauer, B. Jayatilaka, S. Jindariani, M. Johnson, U. Joshi, B. Klima, M.J. Kortelainen, B. Kreis, S. Lammel, J. Lewis, D. Lincoln, R. Lipton, M. Liu, T. Liu, J. Lykken, K. Maeshima, J.M. Marraffino, D. Mason, P. McBride, P. Merkel, S. Mrenna, S. Nahn, V. O'Dell, V. Papadimitriou, K. Pedro, C. Pena, G. Rakness, F. Ravera, L. Ristori, B. Schneider, E. Sexton-Kennedy, N. Smith, A. Soha, W.J. Spalding, L. Spiegel, S. Stoynev, J. Strait, N. Strobbe, L. Taylor, S. Tkaczyk, N.V. Tran, L. Uplegger, E.W. Vaandering, C. Vernieri, M. Verzocchi, R. Vidal, M. Wang, H.A. Weber

University of Florida, Gainesville, USA

D. Acosta, P. Avery, P. Bortignon, D. Bourilkov, A. Brinkerhoff, L. Cadamuro, A. Carnes, V. Cherepanov, D. Curry, F. Errico, R.D. Field, S.V. Gleyzer, B.M. Joshi, M. Kim, J. Konigsberg, A. Korytov, K.H. Lo, P. Ma, K. Matchev, N. Menendez, G. Mitselmakher, D. Rosenzweig, K. Shi, J. Wang, S. Wang, X. Zuo

Florida International University, Miami, USA

Y.R. Joshi

Florida State University, Tallahassee, USA

T. Adams, A. Askew, S. Hagopian, V. Hagopian, K.F. Johnson, R. Khurana, T. Kolberg, G. Martinez, T. Perry, H. Prosper, C. Schiber, R. Yohay, J. Zhang

Florida Institute of Technology, Melbourne, USA

M.M. Baarmand, V. Bhopatkar, M. Hohlmann, D. Noonan, M. Rahmani, M. Saunders, F. Yumiceva

University of Illinois at Chicago (UIC), Chicago, USA

M.R. Adams, L. Apanasevich, D. Berry, R.R. Betts, R. Cavanaugh, X. Chen, S. Dittmer, O. Evdokimov, C.E. Gerber, D.A. Hangal, D.J. Hofman, K. Jung, C. Mills, T. Roy, M.B. Tonjes, N. Varelas, H. Wang, X. Wang, Z. Wu

The University of Iowa, Iowa City, USA

M. Alhusseini, B. Bilki⁵¹, W. Clarida, K. Dilsiz⁶⁸, S. Durgut, R.P. Gandrajula, M. Haytmyradov, V. Khristenko, O.K. Köseyan, J.-P. Merlo, A. Mestvirishvili⁶⁹, A. Moeller, J. Nachtman, H. Ogul⁷⁰, Y. Onel, F. Ozok⁷¹, A. Penzo, C. Snyder, E. Tiras, J. Wetzel

Johns Hopkins University, Baltimore, USA

B. Blumenfeld, A. Cocoros, N. Eminizer, D. Fehling, L. Feng, A.V. Gritsan, W.T. Hung, P. Maksimovic, J. Roskes, M. Swartz, M. Xiao

The University of Kansas, Lawrence, USA

C. Baldenegro Barrera, P. Baringer, A. Bean, S. Boren, J. Bowen, A. Bylinkin, T. Isidori, S. Khalil, J. King, G. Krintiras, A. Kropivnitskaya, C. Lindsey, D. Majumder, W. Mcbrayer, N. Minafra, M. Murray, C. Rogan, C. Royon, S. Sanders, E. Schmitz, J.D. Tapia Takaki, Q. Wang, J. Williams, G. Wilson

Kansas State University, Manhattan, USA

S. Duric, A. Ivanov, K. Kaadze, D. Kim, Y. Maravin, D.R. Mendis, T. Mitchell, A. Modak, A. Mohammadi

Lawrence Livermore National Laboratory, Livermore, USA

F. Rebassoo, D. Wright

University of Maryland, College Park, USA

A. Baden, O. Baron, A. Belloni, S.C. Eno, Y. Feng, N.J. Hadley, S. Jabeen, G.Y. Jeng, R.G. Kellogg, J. Kunkle, A.C. Mignerey, S. Nabili, F. Ricci-Tam, M. Seidel, Y.H. Shin, A. Skuja, S.C. Tonwar, K. Wong

Massachusetts Institute of Technology, Cambridge, USA

D. Abercrombie, B. Allen, A. Baty, R. Bi, S. Brandt, W. Busza, I.A. Cali, M. D'Alfonso, G. Gomez Ceballos, M. Goncharov, P. Harris, D. Hsu, M. Hu, M. Klute, D. Kovalskyi, Y.-J. Lee, P.D. Luckey, B. Maier, A.C. Marini, C. McGinn, C. Mironov, S. Narayanan, X. Niu, C. Paus, D. Rankin, C. Roland, G. Roland, Z. Shi, G.S.F. Stephens, K. Sumorok, K. Tatar, D. Velicanu, J. Wang, T.W. Wang, B. Wyslouch

University of Minnesota, Minneapolis, USA

A.C. Benvenuti[†], R.M. Chatterjee, A. Evans, S. Guts, P. Hansen, J. Hiltbrand, Sh. Jain, S. Kalafut, Y. Kubota, Z. Lesko, J. Mans, R. Rusack, M.A. Wadud

University of Mississippi, Oxford, USA

J.G. Acosta, S. Oliveros

University of Nebraska-Lincoln, Lincoln, USA

K. Bloom, D.R. Claes, C. Fangmeier, L. Finco, F. Golf, R. Gonzalez Suarez, R. Kamalieddin, I. Kravchenko, J.E. Siado, G.R. Snow, B. Stieger

State University of New York at Buffalo, Buffalo, USA

G. Agarwal, C. Harrington, I. Iashvili, A. Kharchilava, C. Mclean, D. Nguyen, A. Parker, J. Pekkanen, S. Rappoccio, B. Roozbahani

Northeastern University, Boston, USA

G. Alverson, E. Barberis, C. Freer, Y. Haddad, A. Hortiangtham, G. Madigan, D.M. Morse, T. Orimoto, L. Skinnari, A. Tishelman-Charny, T. Wamorkar, B. Wang, A. Wisecarver, D. Wood

Northwestern University, Evanston, USA

S. Bhattacharya, J. Bueghly, T. Gunter, K.A. Hahn, N. Odell, M.H. Schmitt, K. Sung, M. Trovato, M. Velasco

University of Notre Dame, Notre Dame, USA

R. Bucci, N. Dev, R. Goldouzian, M. Hildreth, K. Hurtado Anampa, C. Jessop, D.J. Karmgard, K. Lannon, W. Li, N. Loukas, N. Marinelli, I. Mcalister, F. Meng, C. Mueller, Y. Musienko³⁵, M. Planer, R. Ruchti, P. Siddireddy, G. Smith, S. Taroni, M. Wayne, A. Wightman, M. Wolf, A. Woodard

The Ohio State University, Columbus, USA

J. Alimena, B. Bylsma, L.S. Durkin, S. Flowers, B. Francis, C. Hill, W. Ji, A. Lefeld, T.Y. Ling, B.L. Winer

Princeton University, Princeton, USA

S. Cooperstein, G. Dezoort, P. Elmer, J. Hardenbrook, N. Haubrich, S. Higginbotham, A. Kalogeropoulos, S. Kwan, D. Lange, M.T. Lucchini, J. Luo, D. Marlow, K. Mei, I. Ojalvo, J. Olsen, C. Palmer, P. Piroué, J. Salfeld-Nebgen, D. Stickland, C. Tully, Z. Wang

University of Puerto Rico, Mayaguez, USA

S. Malik, S. Norberg

Purdue University, West Lafayette, USA

A. Barker, V.E. Barnes, S. Das, L. Gutay, M. Jones, A.W. Jung, A. Khatiwada, B. Mahakud,

D.H. Miller, G. Negro, N. Neumeister, C.C. Peng, S. Piperov, H. Qiu, J.F. Schulte, J. Sun, F. Wang, R. Xiao, W. Xie

Purdue University Northwest, Hammond, USA

T. Cheng, J. Dolen, N. Parashar

Rice University, Houston, USA

K.M. Ecklund, S. Freed, F.J.M. Geurts, M. Kilpatrick, Arun Kumar, W. Li, B.P. Padley, R. Redjimi, J. Roberts, J. Rorie, W. Shi, A.G. Stahl Leitton, Z. Tu, A. Zhang

University of Rochester, Rochester, USA

A. Bodek, P. de Barbaro, R. Demina, J.L. Dulemba, C. Fallon, T. Ferbel, M. Galanti, A. Garcia-Bellido, J. Han, O. Hindrichs, A. Khukhunaishvili, E. Ranken, P. Tan, R. Taus

Rutgers, The State University of New Jersey, Piscataway, USA

B. Chiarito, J.P. Chou, A. Gandrakota, Y. Gershtein, E. Halkiadakis, A. Hart, M. Heindl, E. Hughes, S. Kaplan, S. Kyriacou, I. Laflotte, A. Lath, R. Montalvo, K. Nash, M. Osherson, H. Saka, S. Salur, S. Schnetzer, D. Sheffield, S. Somalwar, R. Stone, S. Thomas, P. Thomassen

University of Tennessee, Knoxville, USA

H. Acharya, A.G. Delannoy, J. Heideman, G. Riley, S. Spanier

Texas A&M University, College Station, USA

O. Bouhali⁷², A. Celik, M. Dalchenko, M. De Mattia, A. Delgado, S. Dildick, R. Eusebi, J. Gilmore, T. Huang, T. Kamon⁷³, S. Luo, D. Marley, R. Mueller, D. Overton, L. Perniè, D. Rathjens, A. Safonov

Texas Tech University, Lubbock, USA

N. Akchurin, J. Damgov, F. De Guio, S. Kunori, K. Lamichhane, S.W. Lee, T. Mengke, S. Muthumuni, T. Peltola, S. Undleeb, I. Volobouev, Z. Wang, A. Whitbeck

Vanderbilt University, Nashville, USA

S. Greene, A. Gurrola, R. Janjam, W. Johns, C. Maguire, A. Melo, H. Ni, K. Padeken, F. Romeo, P. Sheldon, S. Tuo, J. Velkovska, M. Verweij

University of Virginia, Charlottesville, USA

M.W. Arenton, P. Barria, B. Cox, G. Cummings, R. Hirosky, M. Joyce, A. Ledovskoy, C. Neu, B. Tannenwald, Y. Wang, E. Wolfe, F. Xia

Wayne State University, Detroit, USA

R. Harr, P.E. Karchin, N. Poudyal, J. Sturdy, P. Thapa, S. Zaleski

University of Wisconsin - Madison, Madison, WI, USA

J. Buchanan, C. Caillol, D. Carlsmith, S. Dasu, I. De Bruyn, L. Dodd, F. Fiori, C. Galloni, B. Gombler⁷⁴, M. Herndon, A. Hervé, U. Hussain, P. Klabbers, A. Lanaro, A. Loeliger, K. Long, R. Loveless, J. Madhusudanan Sreekala, T. Ruggles, A. Savin, V. Sharma, W.H. Smith, D. Teague, S. Trembath-reichert, N. Woods

†: Deceased

1: Also at Vienna University of Technology, Vienna, Austria

2: Also at IRFU, CEA, Université Paris-Saclay, Gif-sur-Yvette, France

3: Also at Universidade Estadual de Campinas, Campinas, Brazil

4: Also at Federal University of Rio Grande do Sul, Porto Alegre, Brazil

5: Also at UFMS, Nova Andradina, Brazil

6: Also at Universidade Federal de Pelotas, Pelotas, Brazil

- 7: Also at Université Libre de Bruxelles, Bruxelles, Belgium
- 8: Also at University of Chinese Academy of Sciences, Beijing, China
- 9: Also at Institute for Theoretical and Experimental Physics named by A.I. Alikhanov of NRC 'Kurchatov Institute', Moscow, Russia
- 10: Also at Joint Institute for Nuclear Research, Dubna, Russia
- 11: Also at Cairo University, Cairo, Egypt
- 12: Also at Zewail City of Science and Technology, Zewail, Egypt
- 13: Also at Purdue University, West Lafayette, USA
- 14: Also at Université de Haute Alsace, Mulhouse, France
- 15: Also at Erzincan Binali Yildirim University, Erzincan, Turkey
- 16: Also at CERN, European Organization for Nuclear Research, Geneva, Switzerland
- 17: Also at RWTH Aachen University, III. Physikalisches Institut A, Aachen, Germany
- 18: Also at University of Hamburg, Hamburg, Germany
- 19: Also at Brandenburg University of Technology, Cottbus, Germany
- 20: Also at Institute of Physics, University of Debrecen, Debrecen, Hungary, Debrecen, Hungary
- 21: Also at Institute of Nuclear Research ATOMKI, Debrecen, Hungary
- 22: Also at MTA-ELTE Lendület CMS Particle and Nuclear Physics Group, Eötvös Loránd University, Budapest, Hungary, Budapest, Hungary
- 23: Also at IIT Bhubaneswar, Bhubaneswar, India, Bhubaneswar, India
- 24: Also at Institute of Physics, Bhubaneswar, India
- 25: Also at Shoolini University, Solan, India
- 26: Also at University of Visva-Bharati, Santiniketan, India
- 27: Also at Isfahan University of Technology, Isfahan, Iran
- 28: Also at Italian National Agency for New Technologies, Energy and Sustainable Economic Development, Bologna, Italy
- 29: Also at Centro Siciliano di Fisica Nucleare e di Struttura Della Materia, Catania, Italy
- 30: Also at Scuola Normale e Sezione dell'INFN, Pisa, Italy
- 31: Also at Riga Technical University, Riga, Latvia, Riga, Latvia
- 32: Also at Malaysian Nuclear Agency, MOSTI, Kajang, Malaysia
- 33: Also at Consejo Nacional de Ciencia y Tecnología, Mexico City, Mexico
- 34: Also at Warsaw University of Technology, Institute of Electronic Systems, Warsaw, Poland
- 35: Also at Institute for Nuclear Research, Moscow, Russia
- 36: Now at National Research Nuclear University 'Moscow Engineering Physics Institute' (MEPhI), Moscow, Russia
- 37: Also at St. Petersburg State Polytechnical University, St. Petersburg, Russia
- 38: Also at University of Florida, Gainesville, USA
- 39: Also at Imperial College, London, United Kingdom
- 40: Also at P.N. Lebedev Physical Institute, Moscow, Russia
- 41: Also at California Institute of Technology, Pasadena, USA
- 42: Also at Budker Institute of Nuclear Physics, Novosibirsk, Russia
- 43: Also at Faculty of Physics, University of Belgrade, Belgrade, Serbia
- 44: Also at Università degli Studi di Siena, Siena, Italy
- 45: Also at INFN Sezione di Pavia ^a, Università di Pavia ^b, Pavia, Italy, Pavia, Italy
- 46: Also at National and Kapodistrian University of Athens, Athens, Greece
- 47: Also at Universität Zürich, Zurich, Switzerland
- 48: Also at Stefan Meyer Institute for Subatomic Physics, Vienna, Austria, Vienna, Austria
- 49: Also at Adiyaman University, Adiyaman, Turkey
- 50: Also at Şırnak University, Sirnak, Turkey

-
- 51: Also at Beykent University, Istanbul, Turkey, Istanbul, Turkey
 - 52: Also at Istanbul Aydin University, Istanbul, Turkey
 - 53: Also at Mersin University, Mersin, Turkey
 - 54: Also at Piri Reis University, Istanbul, Turkey
 - 55: Also at Gaziosmanpasa University, Tokat, Turkey
 - 56: Also at Ozyegin University, Istanbul, Turkey
 - 57: Also at Izmir Institute of Technology, Izmir, Turkey
 - 58: Also at Marmara University, Istanbul, Turkey
 - 59: Also at Kafkas University, Kars, Turkey
 - 60: Also at Istanbul Bilgi University, Istanbul, Turkey
 - 61: Also at Hacettepe University, Ankara, Turkey
 - 62: Also at School of Physics and Astronomy, University of Southampton, Southampton, United Kingdom
 - 63: Also at IPPP Durham University, Durham, United Kingdom
 - 64: Also at Monash University, Faculty of Science, Clayton, Australia
 - 65: Also at Bethel University, St. Paul, Minneapolis, USA, St. Paul, USA
 - 66: Also at Karamanoğlu Mehmetbey University, Karaman, Turkey
 - 67: Also at Vilnius University, Vilnius, Lithuania
 - 68: Also at Bingol University, Bingol, Turkey
 - 69: Also at Georgian Technical University, Tbilisi, Georgia
 - 70: Also at Sinop University, Sinop, Turkey
 - 71: Also at Mimar Sinan University, Istanbul, Istanbul, Turkey
 - 72: Also at Texas A&M University at Qatar, Doha, Qatar
 - 73: Also at Kyungpook National University, Daegu, Korea, Daegu, Korea
 - 74: Also at University of Hyderabad, Hyderabad, India